GODDARD GRANT
IN-47-CR
130107
56P.

DESIGN OF THE PRIMARY PRE-TRMM
AND TRMM GROUND TRUTH SITE

Annual Report

NASA Grant #NAG-5-870

(NASA-CR-182609) DESIGN OF THE PRIMARY PRE-TRMM AND TRMM GROUND TRUTH SITE Annual Report (Virginia Univ.) 56 p CSCL 04B

N88-19865

Unclas
G3/47 0130107

DESIGN OF THE PRIMARY PRE-TRMM AND TRMM GROUND TRUTH SITE

Annual Report

on

NASA Grant #NAG-5-870

Submitted by

Michael Garstang
Principal Investigator

University of Virginia
Department of Environmental Sciences
Charlottesville, VA 22903

1 April 1988

1. Introduction

Work began on the design of the primary Pre-TRMM and TRMM ground truth sites under NASA Grant #NAG-5-870 on February 15, 1987. The primary objectives of the work were to:

a) integrate the rain gage measurements with radar measurements of rainfall using the KSFC/Patrick digitized radar and associated rainfall network.

b) delineate the major rain bearing systems over Florida using the Weather Service reported radar/rainfall distributions.

c) combine a) and b).

d) use c) to represent patterns of rainfall which actually exist AND contribute significantly to the rainfall to test sampling strategies. Based on the results of these analyses decide upon the ground truth network.

e) complete the design begun in Phase I of a multi-scale (space and time) surface observing precipitation network centered upon KSFC.

2. Work Accomplished

2.1 Patrick/KSFC Radar

A digital system with associated computer and display equipment has been installed at Patrick and at the Cape Canaveral Forecast Center. The digitized radar record is now being transferred on magnetic tape to the Goddard Laboratory for Atmospheric Science and to the McGill Radar Weather Observatory. These data are being compared with the rainfall measurements from the rain gage network installed within the range of the Patrick radar and will form part of the data base for analysis.

2.2 Cape Canaveral Rain Gage Network

Digital recording rain gage sites have been located on Cape Canaveral and an initial array of rain gages have been installed (Fig. 1). Instruments and recorders have been obtained to equip a wider network within the useful range of the Patrick radar. These gages will be installed during the next period of funding. Appendix I describes the digital recording rain gage system being installed.

2.3 Other Data

Florida rainfall data for the period 1971-1986 has been obtained for $\sim$ 30 recording gages (15 min totals) and 1942-1986 for $\sim$ 80 recording stations (hourly totals). Digital radar data for Florida has also been obtained for a 9-year period (1978-87). Appendix II contains detail on the Florida historical rainfall record.

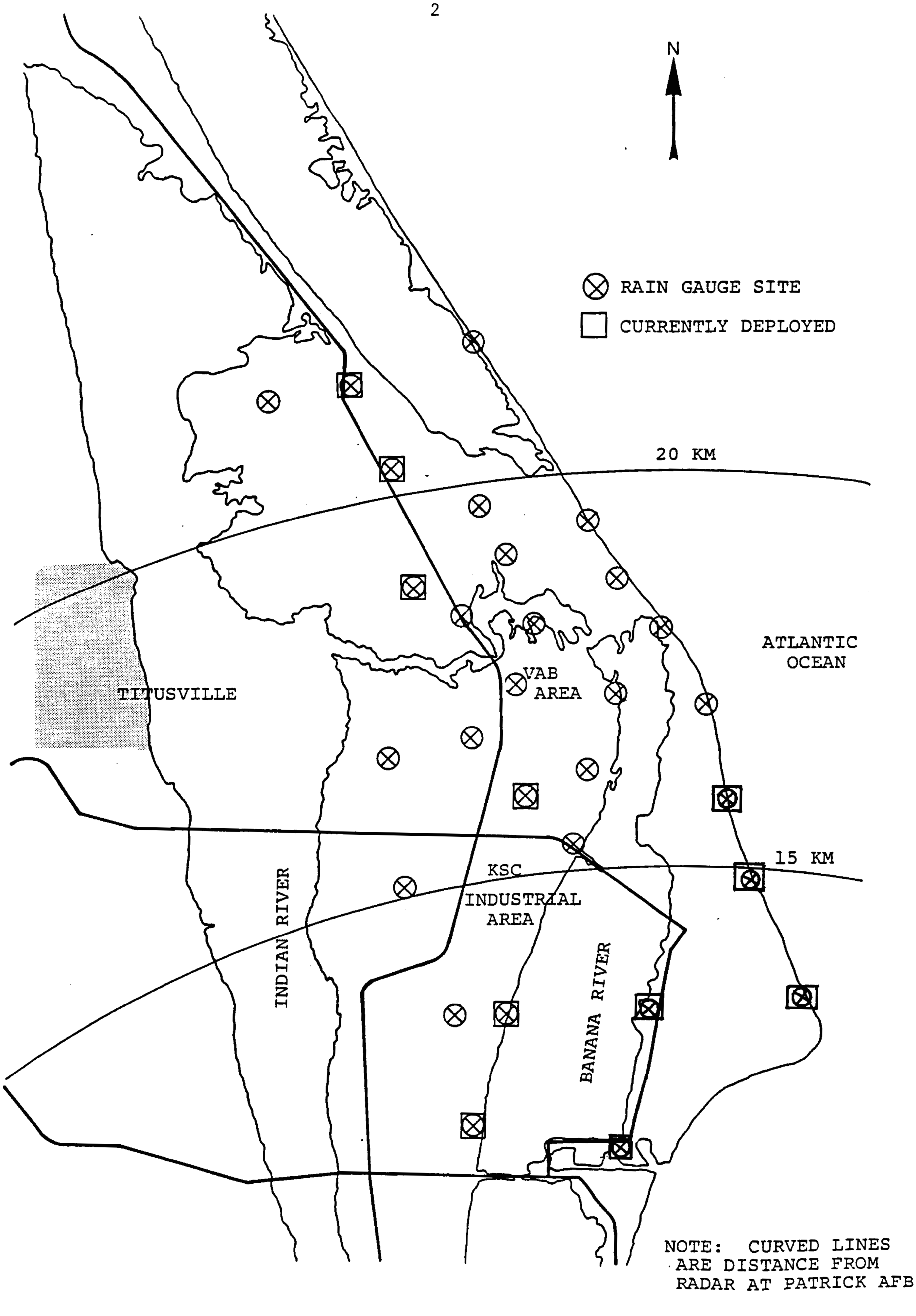
N
RAIN GAUGE SITE
CURRENTLY DEPLOYED
20 KM
15 KM
ATLANTIC
OCEAN
TITUSVILLE
VAB
AREA
KSC
INDUSTRIAL
AREA
INDIAN RIVER
BANANA RIVER
NOTE: CURVED LINES
ARE DISTANCE FROM
RADAR AT PATRICK AFB

Contact has been made with the South Florida and the St. John's River Water Management Districts. A large amount of recording rain gage data is on file at the South Florida Water Management District. Plans are in progress to determine what of the Water Management District's (WMD) data needs to be acquired and where supplemental gages should be sited.

2.4 Analyses Completed and Reported Upon

Analysis of rain gage, radar and satellite estimates of rainfall was reported upon in the Proceedings of the Tokyo International Symposium on Tropical Rainfall held in October 1987 (Austin, 1987, copy attached).

Estimation of tropical rainfall with emphasis upon convective and stratiform rainfall is also reported on in the same proceedings (Garstang et al., 1987, copy attached).

3. Work in Progress

3.1 Estimation of Errors in Area Average Rainfall: Small Scale (McGill)

Considerable uncertainty exists in the estimation of the areal average rainfall. The errors in areal rainfall estimation are more severe when the rainfall is convective in nature. Furthermore, a knowledge of the error vs rain gage network density is important in the assessment of remote sensing of rainfall measurement schemes and the design of the TRMM ground truth network. We are, therefore, continuing to address the relationship between rain gage density, network geometry and the likely error in estimating the areal average rainfall. We are addressing this problem on the small and large scale. The small scale equates to the area covered by the radar, the large scale to that of the peninsula of Florida.

3.1.1 Data base

The following will be used in the analysis.

3.1.1.1 Radar data

Kennedy Space Flight Center radar data covering the period 5 August 1987 to 30 August 1987 will be used to create CAPPIs at five minute intervals. The CAPPI will cover a 480 km square using a pixel size of four square kilometers. The CAPPI altitude will be 3000 m. These 5 minute CAPPIs will be combined to produce total rainfall maps for the following accumulation periods: 15 min, 30 min, 1 hr, 2 hr, 4 hr, 8 hr, 12 hr, 24 hr, 2 days, 4 days, 7 days, 14 days and 25 days.

3.1.1.2 Rain gage data

The rain gage data consists of hourly or daily rainfall totals. These data will be used to calibrate the Z-R relationship used in the generation of the rainfall maps.

3.1.2 Data analysis

The rainfall maps produced in the first phase of the research program will be assumed to be error free maps of rainfall that could have fallen. These maps will therefore be used as "truth" in the analysis that follows.

3.1.2.1 Mean areal rainfall

The rainfall maps will be sampled at random positions to simulate rain gage networks of various densities. Two types of networks viz. random spacing and grid networks, will be used. The error in the areal average rainfall for various size "catchments" will be calculated for each rain gage network. Variables such as the orientation of the network and spacing in the two orthogonal directions will be explored.

3.1.2.2 Volume and areal extent of individual storms

Standard interpolation techniques will be used to calculate the volume of rainfall and areal extent of individual storms using the various rain gage network densities. The actual volume and area of each storm will be calculated and an error versus network density will be plotted for both the area and the volume.

3.1.2.3 Statistical structure

The correlation versus distance function will be calculated for both the radar data and the rain gage data. Of particular interest is the estimated length of the decorrelation distance as a function of the number of rain gages. In addition, the log accumulative results will be tabulated *ala* Lovejoy to test the fractal modeling hypothesis.

3.2 Estimation of Errors in Area Average Rainfall: Large Scale (University of Virginia)

Peninsula scale distributions of rainfall have been determined from manually digitized hourly radar data. The time period covered is June, July and August 1978-1982. The area of investigation encompasses the Florida peninsula and at least 50 km of adjacent ocean. The manually digitized radar (MDR) cells varied between 36-38 km resolution depending on latitude. A total of 150 cells were analyzed and decomposed into principal components to identify the spatial patterns of the daily rainfall regime. A total of 9 years of digitized data is available to extend this initial analysis based on about 9000 hours.

The objective is to first determine the character of the "major" rain bearing systems over Florida. We will define a "major" rain bearing system in terms of the contribution of that system to the summer seasonal rainfall of south Florida.

Having defined and identified the major rain bearing systems we will determine the time and space distributions of the radar estimated rainfall as shown by the operational network. We will then examine the detailed distributions of echoes from a selected few storms from single radars including the Patrick radar.

The most reasonable distributions of rainfall in time and space for the major bearing systems will then be constructed.

Once constructed these distributions will be tested against past observed rainfall from rain gages. This comparison will be used to establish a measure of what is meant by a reasonable distribution.

The resulting distributions will then be regarded as "real" distributions and will be used in simulations to develop the optimum distribution of ground truth measurements.

3.3 Estimation of Errors in Area Average Rainfall: Small scale (McGill)

3.3.1 Basic data processing

Kennedy Space Center radar data for 8th to 30th August 1987 have been processed to form a single data base of approximately 2000 CAPPIs at 3 km altitude. The raw data tapes were first read to produce a data base consisting of the raw DVIP values for each 5 minute CAPPI in polar coordinates. These data were transformed into rainfall amounts by means of

$$Z = 200 * R \exp (1.6)$$

The rainfall amounts were then mapped onto a Cartesian coordinate system with a grid spacing of 2 km by 2 km.

It is important to note that in making the CAPPI map all of the polar data points falling in the Cartesian pixels were correctly averaged as rainfall rates. The resulting maps were interpreted as if they were true rainfall rates based on the electrical calibration of the radar without being calibrated against the existing gage network. This was mainly due to the difficulty in obtaining the very sparse gage data. However, it is hoped that these experiments will be repeated using improved radar data for June, July and August of 1988 with the now much improved gage network in place. For the present study we will argue that while the radar data may not represent the actual rainfall which fell during August 1987, it is a plausible realization of the same random process, and therefore, has the same statistical structure. Since our "gage data" is actually sampled from the radar data, there is clearly no possibility of a gage/radar calibration error in the statistical analysis.

An interactive editing program was written so as to enable strict quality control on the 5 minute CAPPI data. A significant amount of echo was determined to be ground echo, anomalous propagation and interference and was thus removed. The editing of the entire data base is now substantially complete. During this phase of the work it became apparent that on average 15 minutes of data were missing per hour recorded. A simple procedure was written to calculate the movement of the rain area over the missing period. The CAPPIs at either end of the gap were then offset by an appropriate amount and used to fill gaps of less than 20 minutes. The quality of an otherwise excellent data set was compromised by these gaps, and it is hoped that they be eliminated from the next summer's data.

3.3.2 Basic statistical description of the data

A basic statistical package was written to calculate the following statistics for each CAPPI in the data base:

1. mean areal rainfall,
2. mean rainfall depth,
3. variance of the rainfall,
4. rain area,
5. histogram of rainfall amounts,
6. variogram for rainfall in the north/south direction,
7. variogram for rainfall in the east/west direction.

3.3.3 A first look at sampling errors in rain gage networks

The data base was searched for two periods of reasonably intense convective activity. The first period chosen was the 12th August 1987. The 5-minute data were accumulated to give 18 one-hour accumulations. This period included a three hour period of very small, intense rainfall and thus would produce errors that could plausibly represent a worst case situation. The second period was the 29th August 1987. The set consisted of 15 one-hour accumulations representing moderate convective activity.

3.3.3.1 Selection of gage to rainfall map interpolation method

It was thought *a priori* that some form of Kriging technique would be the most suitable interpolation method. The average variograms for the two periods were therefore calculated and reproduced in Figs. 2 and 3. It is immediately apparent from these figures that, given that it is raining at both locations, hourly rainfall depths are independent at distances exceeding approximately 8 km. Therefore, Kriging, which relies heavily on interstation correlations, would not yield anything more obviously useful than say Thiessen polygons which, at least, have the virtue of being easy to compute. Thiessen polygons were, therefore, selected as the method of interpolation from the random gage network to the regular map grid. The accuracy of the various interpolation schemes will be analyzed in more detail later.

3.3.3.2 Simulation method

A uniformly random gage network was created and used to calculate the standard mean interpolation error for the mean areal rainfall, mean depth of rain and rain area. The gage positions were not allowed to be less than 8 km apart in this simulation. A total of 10 different random networks for the 29th August data and 13 networks for the 12th August data were used in the simulation. The mean and standard deviation of the mean standard error for all the networks combined was calculated for each data set using networks with 400, 600, 800, 1000 and 1200 gages covering an area of 124,400 square km. The simulation method will be repeated

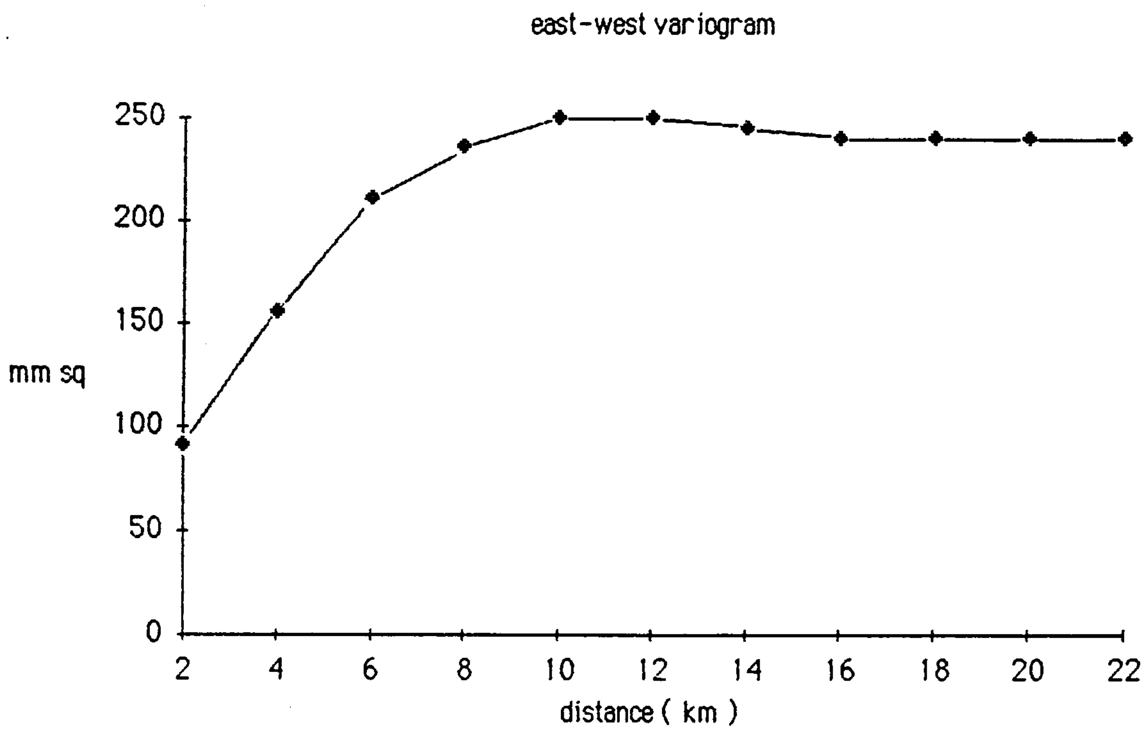

Figure 2. Variogram for the 1-hour accumulation patterns for the 29th August 1987.

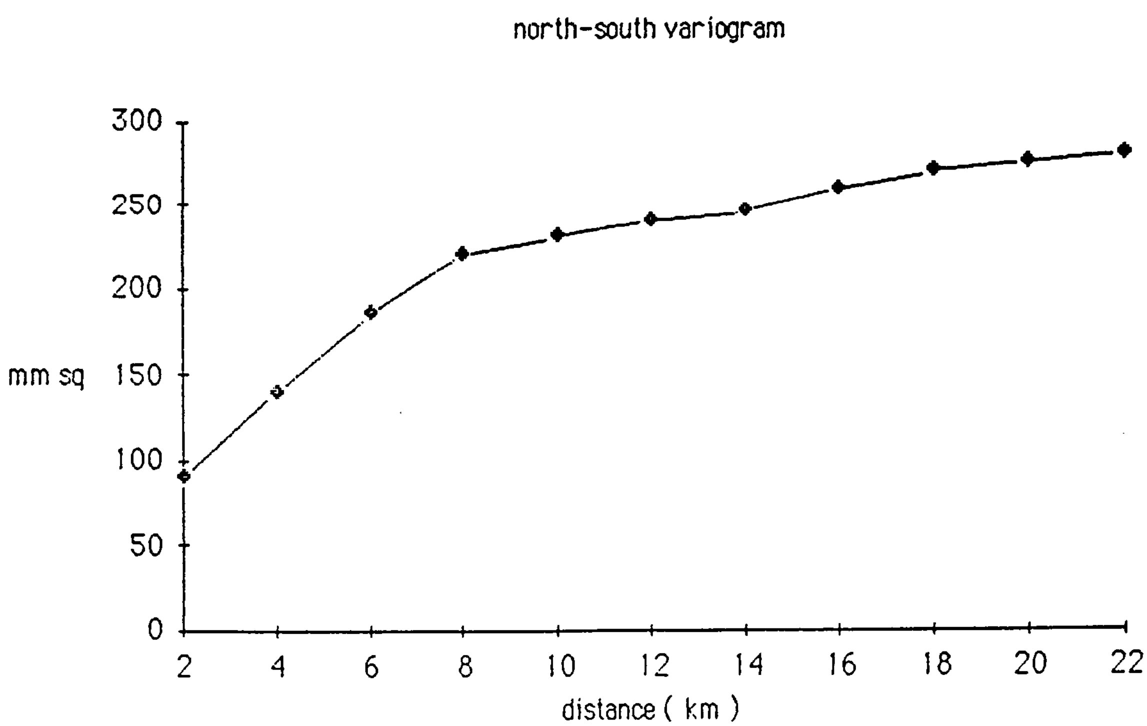

Figure 3. Variogram for the 1-hour accumulation patterns for the 29th August 1987.

using rectangular and triangular networks of gages at different orientations.

3.3.3.3 Some preliminary results

The mean and standard deviations of the standard error for the areal rainfall, mean rain depth and rain area estimates are found in Figs. 4, 5 and 6, respectively for the 12th August data and in Figs. 7, 8 and 9, respectively for the 29th August data. The rain gage networks were found to be able to estimate the areal extent of the rainfall fairly well, the error for the 400 gage network was approximately 10 percent for both of the data sets. However, the same cannot be said for the rain gage estimation of the mean rainfall depth where the errors for the 400 gage network were of the order of 40 percent for the 29th August and 90 percent for the 12th August. Most of the error for the 12th August can be attributed to the three-hour period of intense local convection storms. The error in the areal mean rainfall is approximately 25 percent for the 400 gage network for both data sets. These results illustrate the extremely large errors produced by even relatively dense gage networks, particularly for convective rainfall. It is against these errors that the various remote sensing techniques have to be evaluated.

3.4 Future Work

The results presented above should be extended into the following areas.

3.4.1 Longer accumulation periods and other data sets

The above analysis will be repeated using longer accumulation times and other data sets within the Kennedy Space Center data base and from other radar sites particularly a South African 28°S semi-arid location.

3.4.2 Variogram sampling errors using rain gages

The rain gage network underestimates the variance of the rainfall process. The effect of this underestimation on the variogram constructed from rain gage data needs to be assessed. Errors in this part of the normally preferred Kriging analysis may lead to overly optimistic error estimates for gage estimated rainfall fields.

3.4.3 The effect of radar introduced noise

The above analysis assumed that the rain fields found in nature were accurately represented by the radar data. However, it is possible that the radar based rain fields are more noisy than the true rain fields which occur in nature and therefore, the results of this experiment will be unduly pessimistic. This possibility can be investigated by testing the effects of adding artificial noise and of smoothing the radar fields.

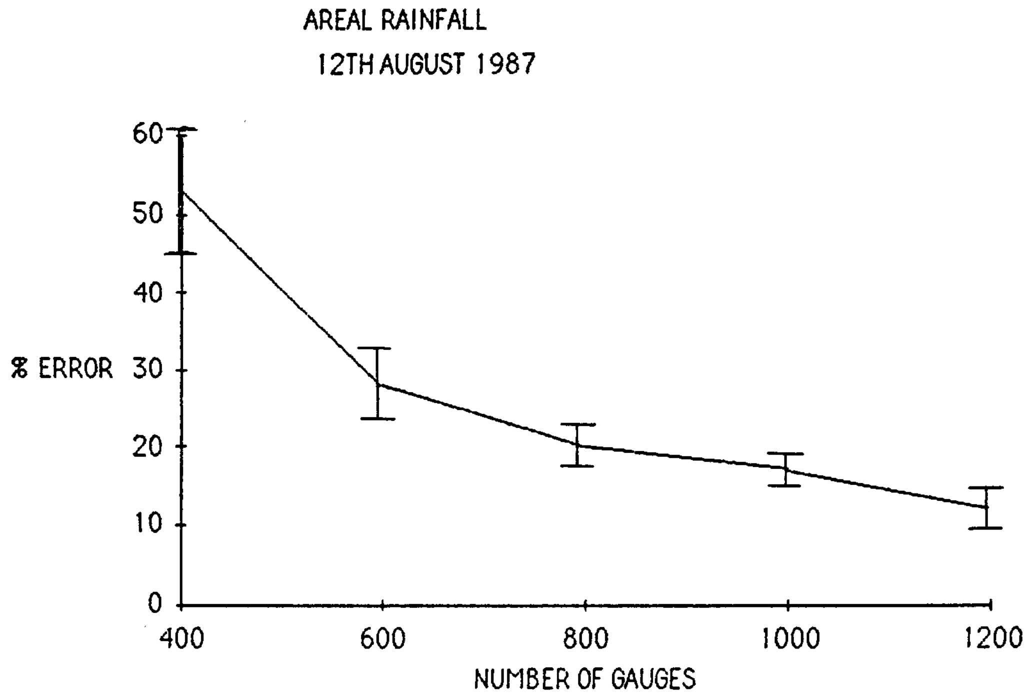

Figure 4. Mean and standard deviation of the error of the areal rainfall estimate (12th August 1987).

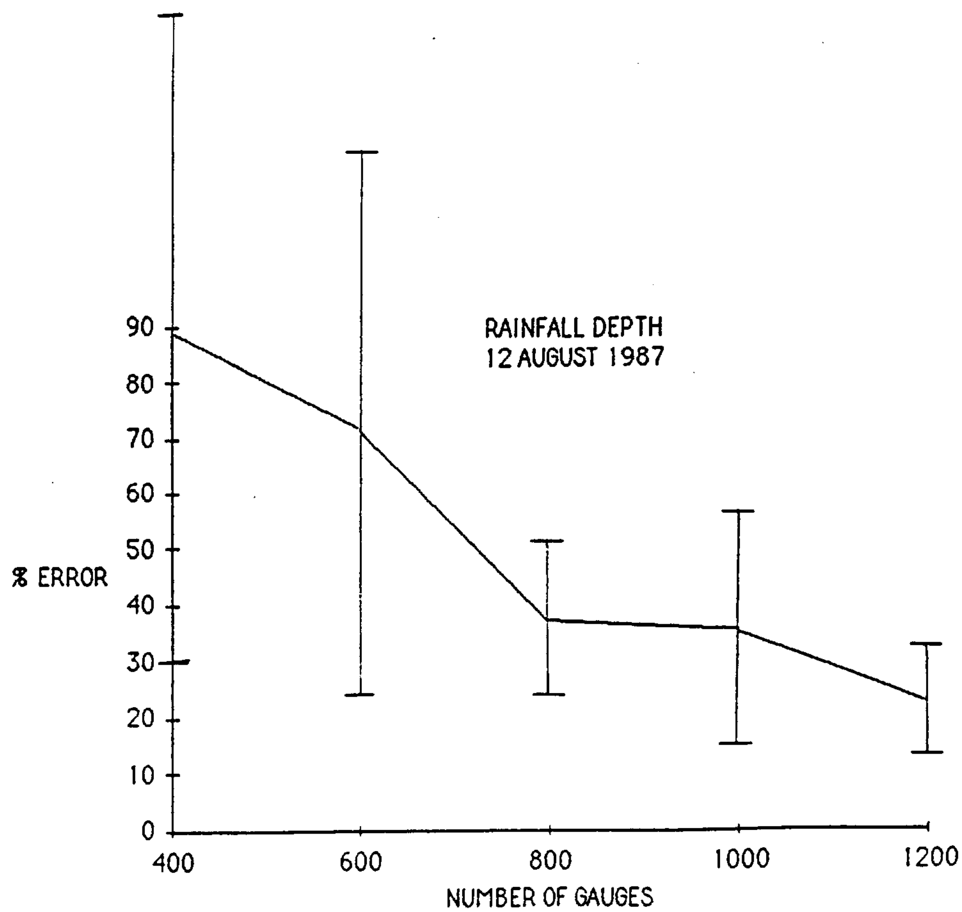

Figure 5. Mean and standard deviation of the error of the rain depth estimate (12th August 1987).

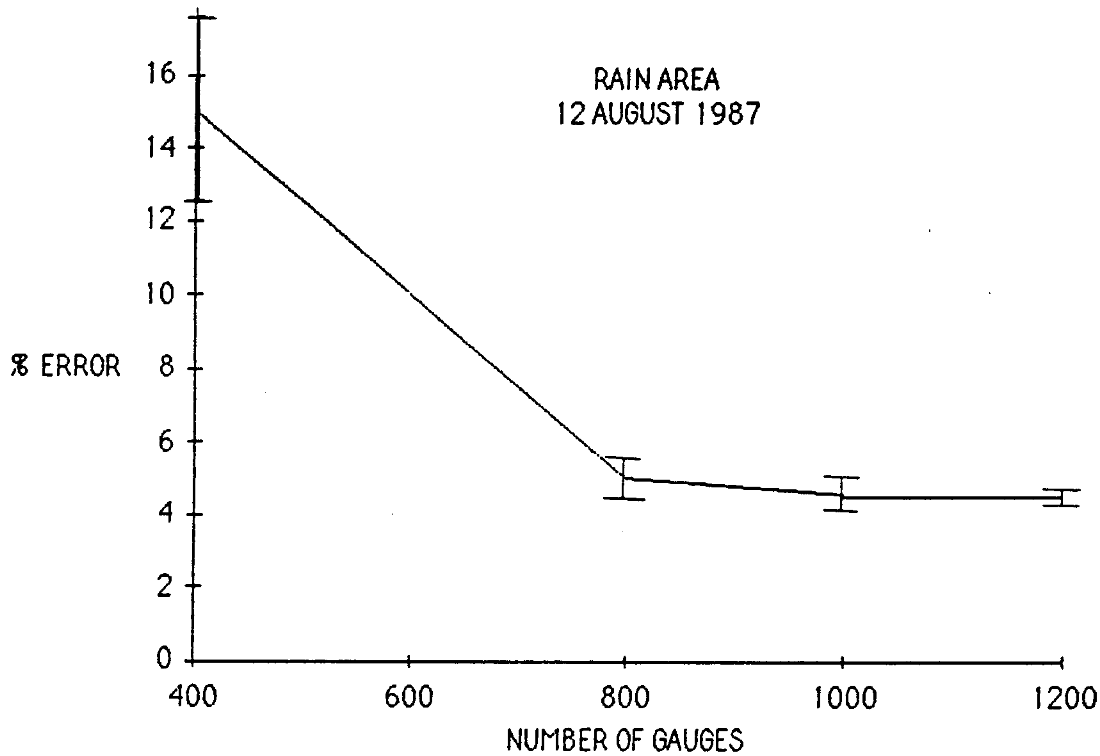

Figure 6. Mean and standard deviation of the error of the rain area estimate (12th August 1987).

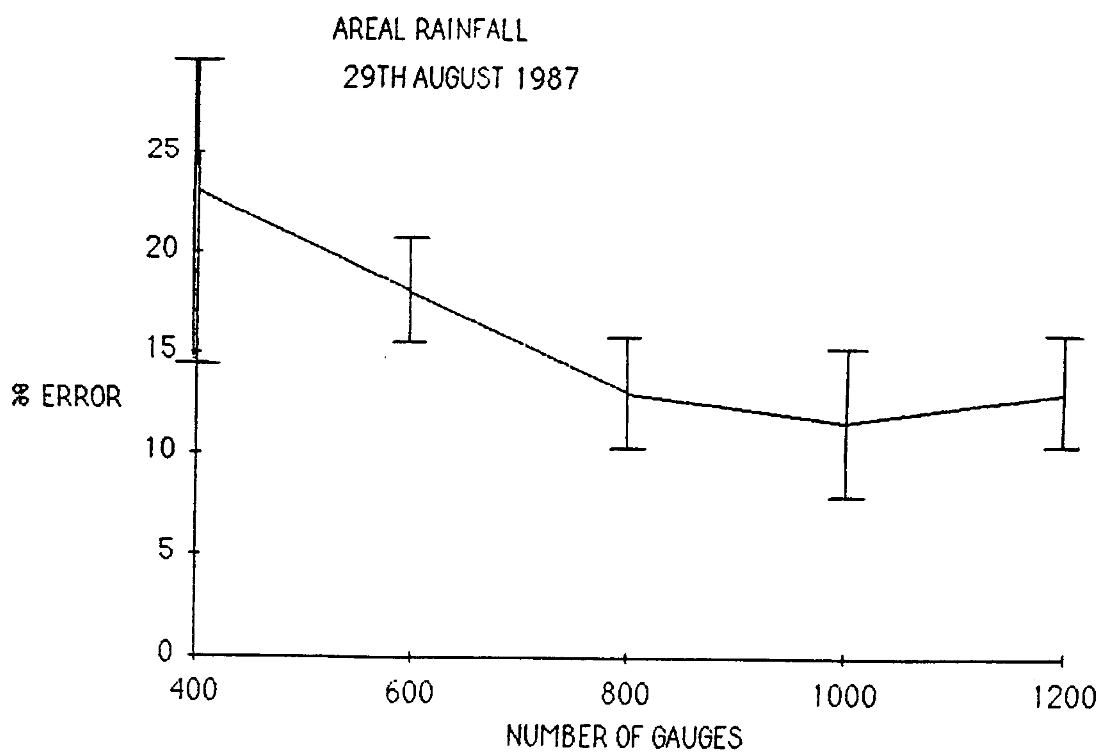

Figure 7. Mean and standard deviation of the error of the areal rainfall estimate (29th August 1987).

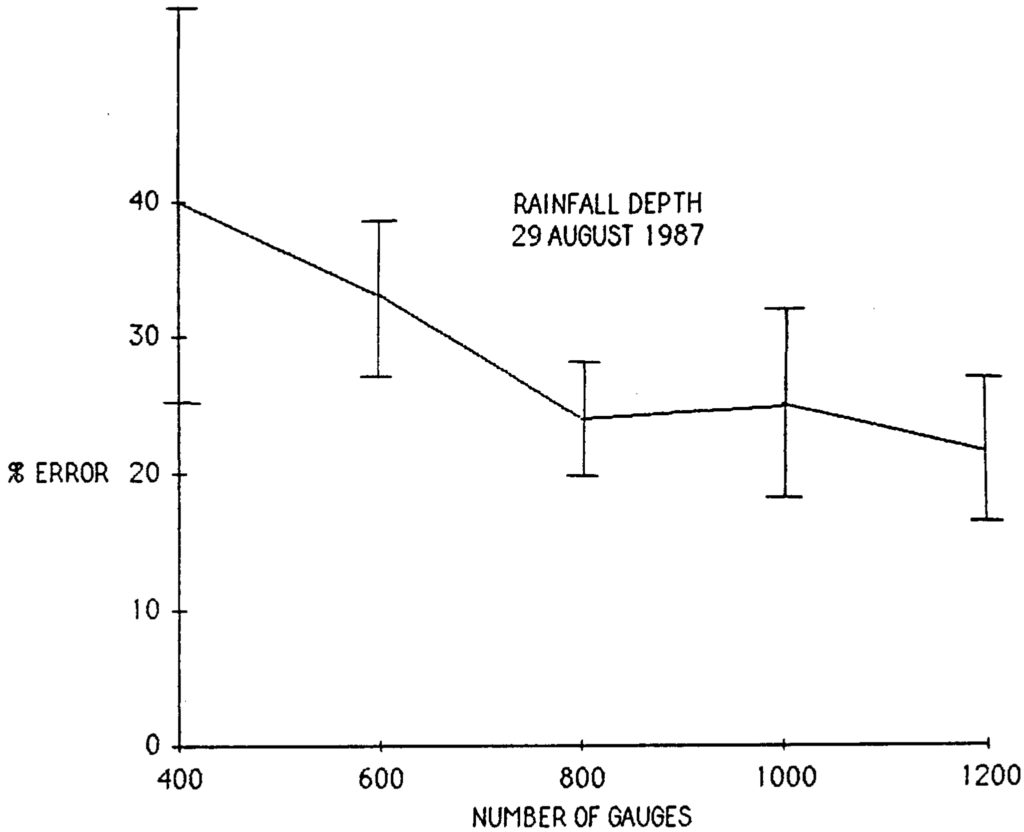

Figure 8. Mean and standard deviation of the error of the rain depth estimate (29th August 1987).

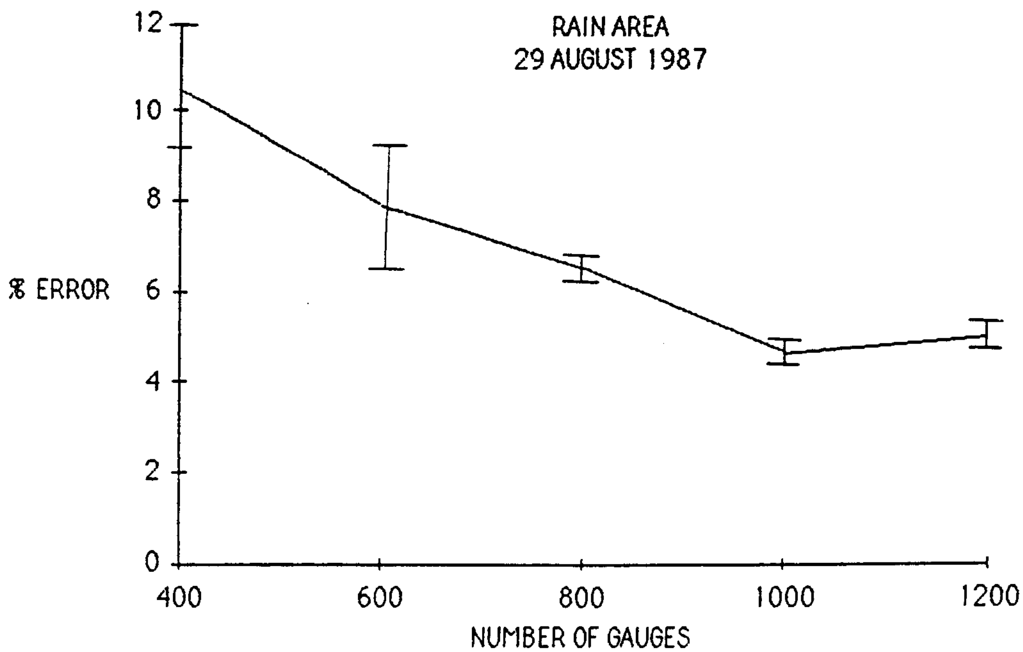

Figure 9. Mean and standard deviation of the error of the rain area estimate (29th August 1987).

3.4.4 An evaluation of the TRMM sampling scheme

The likely errors resulting from the proposed TRMM sampling scheme will be evaluated using the Kennedy Space Center data and a data set of semi-arid subtropical rainfall from South Africa.

4. Concluding Remarks

Work will continue in the Florida area to

* improve the surface networks and the Patrick radar,
* examine the potential of existing networks for both historical as well as current data,
* assess the Tampa radar and determine how it can be utilized,
* explore the possibility of using a radar at West Palm Beach and the possibility of installing a radar at Ft. Myers.

Radars at Patrick AFB, Tampa, Ft. Myers and West Palm Beach would provide a detailed mapping of precipitation distributions over a 200x200 km land area and a 400x400 km land-sea area.

Work will also begin on the other ground truth sites at Kwajelein, Thailand and Australia (at Darwin). Data from radar in Darwin has already been received at Goddard.

Begin typing here. You may type ...

ON THE COMBINING OF RAINGAUGE, RADAR AND SATELLITE ESTIMATES OF RAINFALL

G. L. Austin
McGill Radar Weather Observatory
Box 241, Macdonald College
Ste. Anne de Bellevue, Que
Canada H9X 1C0

ABSTRACT

Extreme spatial and temporal variability in the observed rainfall fields suggests that great care needs to be exercised in the calibration of rainfall estimating schemes from gauge networks and other surface data. The development of analytical tools to combine several not very precise rainfall estimating techniques to yield optimum rainfall estimates is reviewed. It is concluded that a large data base of simulated 3-D rainfall data, which can be regarded as accurate, is necessary. These data can then be used to obtain the required optimum integration scheme and error estimates based on a knowledge of the physics of the instrumental measuring biases, noise and sampling characteristics.

1. INTRODUCTION

One of the most significant problems associated with the remote sensing of rainfall is the development of strategies to combine data derived from different rainfall measuring techniques to yield the optimum estimate of areal precipitation. An equally urgent and related problem is to estimate the likely impact of sampling, instrumental and interpretational errors in the remote sensed precipitation data.

Some attention has been given to the former as it relates to the combining of raingauge and radar data (e.g., Austin (1987) Harrold et al. (1973) and Wilson and Brandies (1979)). The literature on techniques for the combining of gauge and satellite data is also quite extensive (see Barrett and Martin (1981) for a review).

2. RAINFALL VARIABILITY

Some of these authors have recognized a major problem in dealing with precipitation data sets - the presence of extreme variability and intermittency (Schertzer and Lovejoy (1987)). The effect of this variability is that schemes designed to produce areal rainfall fields have low accuracy, even for quite dense gauge networks, and particularly in convective situations. Damant et al. (1983), for example, obtain errors of approximately 70% for total storm accumulations over a 4,800 km^2 catchment using 10 raingauges. Bellon and Austin (1986) estimate mean point total storm accumulation differences from gauges at different spacing and obtained 60% differences at a distance of 10 km and 100% difference at a separation of 100 km.

These results have considerable impact on the accuracy with which a remote sensing rainfall measuring system can be calibrated with sparse gauge networks. The calibration of large footprint estimating schemes, particularly those having non-linear averaging characteristics with a sparse gauge data set is clearly hazardous. The use of well-calibrated weather radar data with an estimated ± 30% uncertainty over small catchments for storm totals (Austin (1987) and Bellon and Austin (1986)) then becomes particularly attractive. In order to achieve these accuracies in the radar estimates, specific account has to be taken of the temporal sampling errors (frequencies greater than five minutes are sometimes required), and the variability in the parameters of the non-linear relationship between rainfall and radar reflectivity. The author believes that some of the published accuracy claims for satellite rainfall estimating schemes are unduly optimistic, since they are certainly higher than the accuracy with which the rainfall could be estimated by the sparse calibrating gauge network.

The important point is that there is no existing accurate way to measure the space/time distribution of precipitation. This means that THE PROBLEM OF COMBINING RAINFALL ESTIMATES BECOMES ONE OF COMBINING SEVERAL WRONG ESTIMATES OF RAINFALL TO GET A BEST ESTIMATE OF THE TRUE RAINFALL PATTERN.

3. POSSIBLE STRATEGY

Since no direct estimate of the 'correct' value of the rainfall pattern exists, it is not clear that it is possible to devise the optimum strategy nor estimate its accuracy directly from the wrong fields themselves unless we make sure considerable assumptions about the statistical properties of the 'correct' field.

If a rainfall field in space and time which COULD HAVE existed was simulated stochastically, then simulated rainfall estimates based on the known physics of the measuring system can be generated. This accounts, in part at least, for the great deal of activity in recent years directed toward the stochastic modelling of rainfall patterns. This type of activity has resulted recently in a special issue of the Journal of Geophysical Research (August 1987) and even the establishment of a new journal (Journal of Stochastic Hydrology) to discuss the problems.

An alternative strategy, which to some extent avoids the difficulties associated with producing stochastic rainfall models with correct statistical properties, is to take a series of 3-D radar data sets and argue that although they do NOT represent the actual rainfall pattern that existed in space at the indicated time, they DO represent a pattern that COULD HAVE existed. This pattern can then be modified by the theoretically-derived sampling, non-linear integration and noise contamination characteristics inherent in each of the measurement techniques. This procedure has the enormous advantage that since we start from a 'correct' rainfall pattern we can calculate the statistical properties inherent in each of the measurement schemes, and presumably the optimum combining strategies.

The great advantage of the procedure is that no assumptions have to be made about the statistical properties of the rainfall fields except at space and time scales smaller than the resolution of the

ORIGINAL PAGE IS
OF POOR QUALITY

radar (perhaps 1 km and 5 minutes). This is clearly likely to be a much less drastic assumption than those which assume properties of homogeneity and independence on the large scale. Some would argue, however, that much of the observed discrepancy between radar and gauge data is due to real sub-kilometer variability and that in fact the effective area of representativeness for a raingauge is little more than a circle of radius 4". What has to be assumed is that the physics of the rainfall measuring procedure used by the instrument is well understood. This author, at least, believes that to assume we understand the measuring process in our instruments is generally much safer than to make assumptions about the statistical properties of rainfall patterns which have only been poorly measured. This basic concept has already been used in Damant et al. (1983) in the investigation of the sampling errors of raingauges.

4. METHOD

The problem can be set up following the notation used in Krajewski (1987) in his discussion of cokriging. If $X(k)$ is the true rainfall pattern, where k is a position vector, then one of the remote sensed estimates of the rainfall at the point k will be given by:

$$R_k = \frac{1}{A}\int_A F_{Rk}\, X(k)\, dk + \varepsilon_{Rk}$$

where A is the measurement cell area, F_{Rk} is the bias in the estimate, and ε_{Rk} is the random error. On the other hand, the gauge estimate at the points where gauges exist, k' is

$$G_k = F_{Gk}\, X(k') + \varepsilon_{Gk}$$

where F_{Gk} is the gauge bias and ε_{Gk} the sampling noise.

The problem is to find the best estimate $Y^*(k)$, of

$$Y(k) = \frac{1}{A}\int_A X(k)\, dk$$

In the cokriging approach it is normal to now assume a possible solution of the form

$$Y^*(k) = \sum_{i=1}^{N_G} \lambda_{Gi}\, G_i(k') + \sum_{i=1}^{N_R} \lambda_{Ri}\, R_i(k) + \ldots$$

where the λ's are distance weighting functions which may be determined from the data fields.

5. RESULTS

Preliminary results for this type of work have been obtained for summer rainfall patterns in Montreal, where it has been found that more than 5 km from the raingauge a radar estimate of rainfall is more accurate and that more than 40 km from a gauge then a simple VIS/IR threshold technique yields better rain estimates. A substantial quantity of Kennedy Space Centre weather radar data is now being analyzed with a view to finding the appropriate parameters for a more representative tropical rainfall field.

6. CONCLUSIONS

Extreme spatial and temporal variability in rainfall patterns produce considerable problems for the calibration of remote sensed rain estimation schemes, the development of optimum combining systems for several techniques and error analysis. Work on mid-latitude rain patterns in Montreal, for example, give the results that an estimate of rainfall at a point is better made by radar than a gauge about 5 km away and by satellite using a simple VIS/IR thresholding technique if the gauge is more than about 40 km away.

When we consider systems of remote sensing devices such as are proposed in the TRMM satellite, then in order to establish procedures for producing combined estimates of precipitation together with their likely accuracy, a considerable simulation based on large 3-D data sets is required.

REFERENCES

Austin, P.M., 1987: Relationship between measured radar reflectivity and surface rainfall, Mon. Wea. Rev., 115, 1053-1070.

Barrett, E.C. and D.W. Martin, 1981: The use of satellite data in rainfall monitoring, Academic Press, 340 pp.

Bellon, A. and G.L. Austin, 1986: On the relative accuracy of satellite and raingauge rainfall measurements over middle latitudes during daylight hours, J. Climate and Appl. Meteor., 25, 1712-1724.

Damant, C., G.L. Austin, A. Bellon and R.S. Broughton, 1983: Errors in the Thiessen technique for estimating areal rain amounts using weather radar data. J. Hydrol., 62, 81-94.

Harrold, T.W., E.J. English and C.A. Nichols, 1973: The measurement of area precipitation using radar, Weather, 28, 332-338.

Krajewski, W.F., 1987: Cokriging radar-rainfall and rain gage data. J. Geophy. Res., 92, 9571-9580.

Schertzer D. and S. Lovejoy, 1987: Physical modeling and analysis of rain and clouds by anisotropic scaling multiplicative processes, J. Geophys. Res., 92, 9693-9714.

Wilson, J.W. and E.A. Brandies, 1979: Radar measurement of rainfall - A summary, Bull. Amer. Met. Soc., 60, 1048-1058.

ATTACHMENT 2

Proc. International Symposium on Tropical Precipitation Measurements, Tokyo, Japan, 28-30 October 1987

ESTIMATION OF TROPICAL RAINFALL

Michael Garstang, Claire Cosgrove, Robert Swap
and Steven Greco
University of Virginia
Charlottesville, VA 22903 U.S.A.

ABSTRACT

Convective systems produce the bulk of tropical rainfall but are variable in space and time both in terms of the occurrence of the rain system and the nature of the rain in the system itself. A single example of a continental equatorial squall line over the Amazon Basin is used to illustrate the variability in the rainfall rates and amounts for such systems. Convective core rainfall falling at 0.75 mm/min produces 50 to 70% of the rain, the remaining 30 to 50% occurs in multilayered and single layered cloud regions which vary in both space and time for the same system.

1. INTRODUCTION

Tropical rainfall between the latitudes of 30°N and S constitutes a significant part of the global rainfall (Fig. 1). The greater part of the tropical rainfall occurs in organized meso- to synoptic-scale systems but with large spatial and temporal variability. For example, a pervasive result found by many authors (Riehl, 1954), shows that 50% or more of the rainfall falls in about 10% of the time. Convective rain systems which produce an average of $\geq$ 15 mm of rain per station, typically produce more than 60% of the total annual rainfall. But rain systems with high rain rates, producing the large amounts of rainfall, occur only intermittently. This means that we must measure the high rain rates accurately and we must be able to detect and delineate to organized convective meso- to synoptic-scale systems.

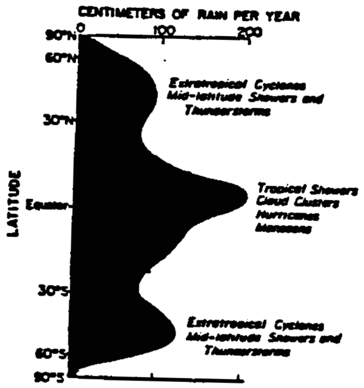

FIGURE 1. Globally averaged annual precipitation and associated rain-producing weather systems. (After Sellers, 1965.)

In this paper, we take the position that organized meso- to synoptic-scale systems as seen over the Amazon Basin of Brazil produce a large fraction of the rainfall of that water rich region. We further wish to establish whether the rainfall characteristics of these equatorial continental systems are similar or dissimilar to their tropical oceanic counterparts.

2. MEASUREMENTS

The NASA Amazon Boundary Layer Experiment (ABLE-2B) (Harriss et al., 1988) made surface meteorological, radar and satellite measurements over the Amazon Basin during the wet season months of April and May 1987. Four Portable Automated Mesonet (PAMs) stations were deployed with sensors on towers approximately 5 m above the canopy of the rain forest. Tipping bucket rain gages at this level measured accumulated rainfall with a resolution of 0.25 mm every minute. The location and spacing of the PAM towers is shown in Fig. 2. Temperature, humidity, pressure, and horizontal wind velocity were also measured at each tower site. Accumulated rainfall (an 8-inch gage) for each rain event was also measured at the surface in a clearing within 3 km of each of the three outer PAM towers.

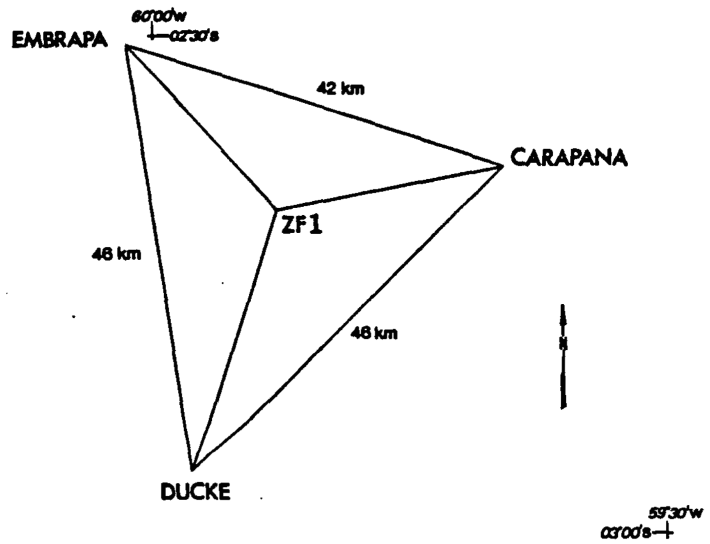

FIGURE 2. Location and spacing of the 4 PAM towers.

A 3 cm radar with digital recording capability was located approximately 15 km SSW of the most southerly PAM tower. GOES (Geostationary Environmental Satellite) satellite imagery (visible and infrared) was collected routinely at Manaus and at the NASA/Langley Research Center in Hampton, VA.

Squall lines, at times up to 3000 km in length, were a relatively frequent phenomena occurring on at least 10 of the 45 days of ABLE-2B. The squall line which passed over the measurement network on the 26th of April 1987 was chosen for this study. The 26th of April system produced a total of 33.02 mm of rain at the Carapana station. Twenty-one rain systems passed across the measurement network in the 45 days of ABLE. The 26th of April ranked 7th and represented 4.51% of the total rain measured over the 45 days.

3. FINDINGS

Figure 3 shows the time distribution of rain amount at each of the 4 recording gage stations. Rain accumulation is plotted every three minutes. The total amount of rain recorded at each station is shown in Table 1. Table 1 also shows the non-recording rain gage amounts and the differences between the recording and non-recording gages.

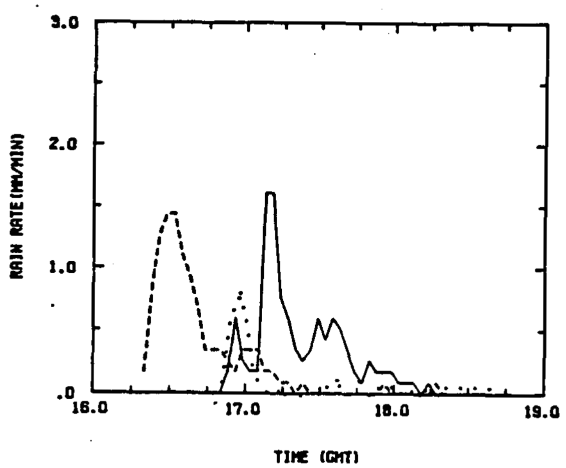

FIGURE 3. Distribution of 3 min totals of rainfall at each of the three perimeter stations: Carapana (dashed), ZF-1 (dotted) and Embrapa (solid).

TABLE 1. TOTAL AMOUNT OF RAIN RECORDED AT EACH STATION

Station	Recording Gage	Non-Recording Gage	% Difference
Carapana	33.02	52.32	37%
Embrapa	32.01	35.30	9%
ZF-1	15.49	-	-
Ducke	0.51	-	-

Figure 4 shows a time series of equivalent potential temperature at the top of the forest canopy. Table 2 compares the time of the θ_e drop with the occurrence of rain at each site. We note that significant θ_e changes are not related to the amount or intensity of measured rainfall but that θ_e drops are always indicative of convective rain process.

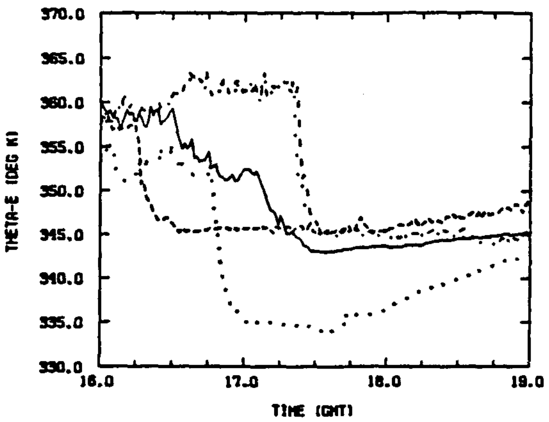

FIGURE 4. Equivalent potential temperature at 5 m above the forest canopy at Carapana (dashed), ZF-1 (dotted), Embrapa (solid) and Ducke (dash-dot).

TABLE 2. COMPARISON OF THE TIME OF θ_e DROP WITH THE OCCURRENCE OF RAIN AT EACH SITE

Station	Time of θ_e Drop	Start of Rain
Carapana	1614 (1.7°K in 1 min)	1616
ZF-1	1647 (2°K in 1 min)	1649
Embrapa	1630 (1.4°K in 1 min)	1651
Ducke	1722 (5°K in 1 min)	1722 (.25 mm)

Figure 5 shows the variability of rainfall intensities at Carapana and Embrapa. At Carapana (Fig. 5a), the greatest variability occurs near the onset of the rain event which coincided with the higher rainfall intensities. The subsequent relative deviations then tend to be similar for both high and low intensities alternating from positive to negative values but within the limits of one standard deviation of the variability. Rain amounts decrease sharply after the vertical dashed line on the abscissa. We note a similar distribution for Embrapa (Fig. 5b) except that we see three distinct regimes separated by variations in intensity and amount. We interpret this change as a change from convective rain to stratiform rain in the sense described by Houze and his collaborators (Houze, 1977; Leary and Houze, 1979; Gamache and Houze, 1982, 1983, 1985; Wei and Houze, 1987). We note in agreement with Smull and Houze (1987) that there is probably a transition zone between the convective and stratiform region of the storm. We do, however, believe that this transition zone is a product of rain from multiple stratiform cloud layers rather than residual convective clouds. We designate this rainfall as a multilayer rainfall and regard it as distinct from the single layer or anvil rainfall which signals the end of the system.

Based upon Fig. 5 and visual inspection of the change in rainfall rates evident in Fig. 3 we select 0.75 mm/min as the boundary between

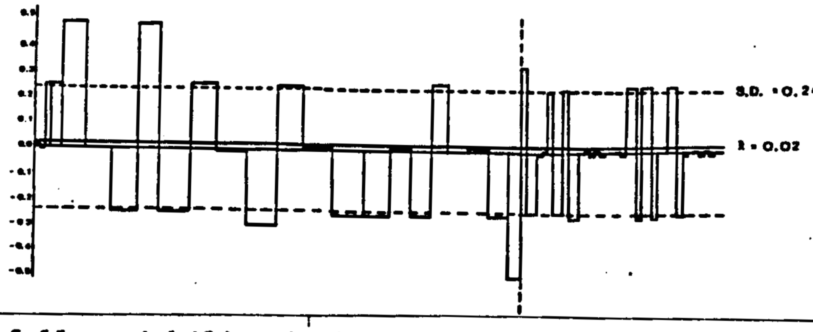

FIGURE 5a. Rainfall variability in intensity and amount is shown for Carapana. Variations in 1 min intensities are shown on the ordinate while the width of the bar shows the amount (or rate x time). The horizontal dashed line represents one standard deviation in intensity.

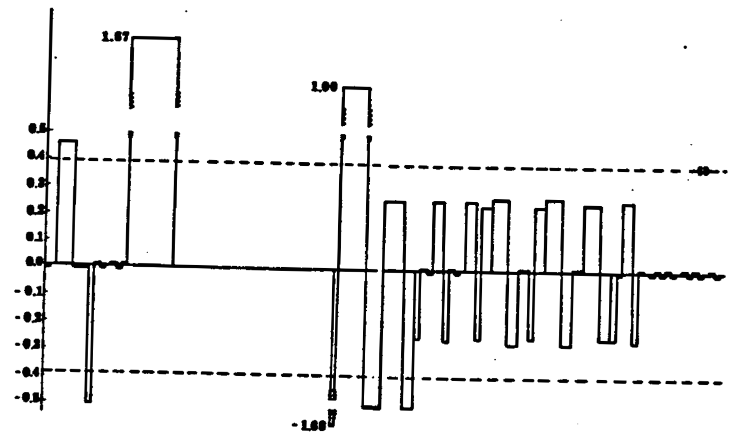

FIGURE 5b. As for Fig. 5a but for Embrapa.

convective and multilayered rainfall, and 0.50 mm/min as the boundary between multilayered and single layer rainfall. Table 3a shows the rainfall at the 0.25 mm/min resolution of the measurement. Table 3b shows the three classes each as a percentage of the total.

TABLE 3a. RAIN RATES AND THE ASSOCIATED PERCENTAGE OF THE TOTAL RAINFALL IN EACH RATE INTERVAL

Station	Total Rain	.25	.50	.75	≥ 1.0
Embrapa	32.01	31.0%	17.4%	14.3%	37.3%
Carapana	33.02	21.6%	10.8%	6.9%	60.7%
ZF-1	15.49	47.5%	9.9%	29.5%	13.1%

The percentage amounts ascribed to the convective class ranges between 40 and 70%, single layered cloud 20 and 50%, the remaining 10 to 20% is placed in the multilayered category.

The forward propagation of the squall line is measured from satellite enhanced infrared images to be 51 kph. The width of the

TABLE 3b. RAIN RATES FOR THE THREE CLASSES OF CONVECTIVE (C $\geq$ .75 mm/min), MULTILAYERED (0.5 $\leq$ M < .75) AND SINGLE LAYERED (S < 0.5)

Station	Total Rain	S	M	C
Embrapa	32.01	31.0%	17.4%	51.6%
Carapana	33.02	21.6%	10.8%	67.6%
ZF-1	15.49	47.5%	9.9%	42.6%

system normal to its direction of propagation as measured from the leading edge to the corresponding grey scale on the opposite side of the squall line remained nearly constant at 290 km.

The width of the precipitating areas can be estimated from the time occupied by the rain rate class multiplied by the speed of propagation of the system. The results are shown in Fig. 6 and summarized in Table 4.

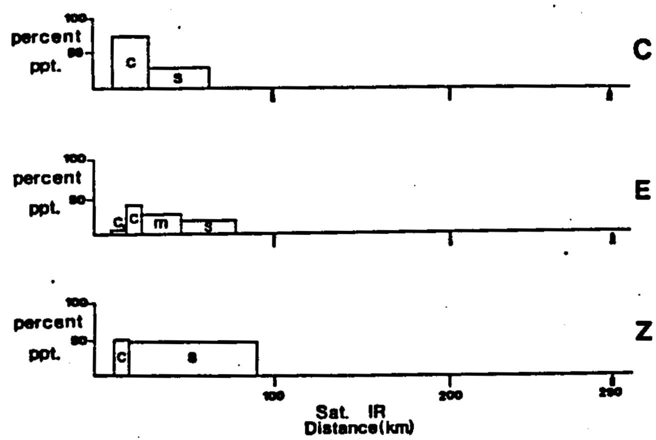

FIGURE 6. Percent of total rain each rain class (C_p = pre-convective, C = convective, M = multilayered, and S = single layered) for each station (C = Carapana, E = Embrapa, and Z = ZF-1). The horizontal axis represents the width of the system (290 km) as obtained from the IR image. The width of each precipitating class is obtained from (time of class rate) x 51 kph.

4. CONCLUSIONS

The rain rates of 0.75 mm/min or greater associated with the convective core of this squall line is significantly higher than rates ascribed to tropical oceanic squall lines (0.25 mm/min). Rates as low as 0.25 mm/min would not appear to correspond to the highly variable region of the squall line where high variability might be equated to convective rainfall.

Spatial variability is also, however, high and at two stations a convective stratiform classification could apply yielding 50 to 70% of

TABLE 4. RAIN DISTRIBUTIONS FROM TIME SPACE CONVERSION

	Pre-Conv	Conv	Multilayered	Single Layered
Carapana	0 km	20.4 km (71%)	0	33.9 km (29%)
Embrapa	8.5 km	8.5 km (41.3%)	22.1 km (33.3%)	29.7 km (29.0%)
ZF-1	0 km	10.2 km (51%)	0	89.1 km (49%)

the rain in the convective region and 30 to 50% in the stratiform region. We believe that the convective core produces between 40 and 70% of the total rainfall.

The remaining 30 to 60% of the rainfall may occur at relatively high rates in the multi-cloud layered region of the storm and at low rates in the single cloud layered region. This variability (30 to 60%) is both spatial and temporal. Any indirect sensing technique employed with the hope of estimating rainfall with an accuracy of greater than 20% will have to deal with these distributions.

5. REFERENCES

Gamache, J.F., and R.A. Houze, Jr., 1982: Mesoscale air motions associated with a tropical squall line. Mon. Wea. Rev., 110, 118-135.

________, and ________, 1983: Water budget of a mesoscale convective system in the tropics. J. Atmos. Sci., 40, 1835-1850.

________, and ________, 1985: Further analysis of the composite wind and thermodynamic structure of the 12 September GATE squall line. Mon. Wea. Rev., 113, 1241-1259.

Harriss, R.C., S.C. Wofsy, M. Garstang, L.C.B. Molion, R.S. McNeal, J. M. Hoell, R.J. Bendura, S.M. Beck, R.L. Navarro, J.T. Riley and R.C. Shell, 1988: The Amazon Boundary Layer Experiment (ABLE). To be published in J. Geophys. Res.

Houze, R.A., Jr., 1977: Structure and dynamics of a tropical squall line system. Mon. Wea. Rev., 105, 1540-1567.

Leary, C.A., and R.A. Houze, Jr., 1979: Melting and evaporation of hydrometeors in precipitation from the anvil clouds of deep tropical convection. J. Atmos. Sci., 36, 669-679.

Riehl, H., 1954: Tropical Meteorology. McGraw-Hill Book Company, Inc., New York, 392 pp.

Smull, B.F., and R.A. Houze, Jr., 1987: Dual-Doppler radar analysis of a midlatitude squall line with a trailing region of stratiform rain. J. Atmos. Sci., 44, 2128-2148.

Wei, T., and R.A. Houze, Jr., 1987: The GATE squall line of 9-10 August 1974. Adv. Atmos. Sci., 4, 85-92.

Type Within Solid Blue Lines

Appendix I

KSC

Raingauge

Network

September 29, 1987

Contents

Hardware

The raingauge hardware is made up of the following components.

Tipping bucket raingauges	Measures rainfall in increments of 0.01".
Raingauge module	The interface between the raingauge and the data cartridge. This small white box fits within the raingauge housing. Each module has an internal serial number which is transferred to the data cartridge when the reset button is pushed.
Data cartridge	This is a small grey cartridge which plugs into the raingauge module. It contains a CMOS memory which is programmed by the module with the time and number of tips registered by the raingauge for a given minute. If no tips occur, no entry is made in the data cartridge. The data cartridge has capacity for approximately 800 entries, or about 8" of rainfall.
Translator	This is the interface used to transfer data from the cartridge to a microcomputer. It can be used either in the field or at the office.
Power inverter (Tripplite)	Used to convert 12 VDC to 120 VAC in order to power the translator in the field. It plugs into an automobile cigar lighter.
Toshiba T1000 personal computer	This is a laptop personal computer which can travel to the field when servicing the raingauge network. It is IBM compatible, and contains a 3 1/2" floppy disk drive. Data from the data cartridge is collected on the T1000's disk. The T1000 contains internal batteries which will provide approximately 4 hours of continuous use between charges.
External 5 1/4" disk drive.	This disk drive connects to the T1000 and is used to copy the 3 1/2" disks to the 5 1/4" standard format.

Software

Software has been provided on both 3 1/2" and 5 1/4" diskettes.

QUEMS Data #1	3 1/2"	This diskette is used to collect the raingauge data. It contains the QUEMS data management software and the DS directory management program.
Misc Software	3 1/2"	Contains copies of QUEMS and DS, as well other software.
NEW_DISK	5 1/4"	Has the QUEMS and DS programs, and the NEW_DISK.BAT batch file. Use this disk to create a new QUEMS Data disk.
NEW_DISK (Copy 2)	5 1/4"	Backup copy of the above.

Data Cartridge Initialization

The following procedure is used to initialize the data cartridge. Begin by connecting the T1000 and the translator, and applying power to both units. The T1000 will go through the boot-up process; when this has finished the C> prompt will be displayed.

1. Put the QUEMS/data disk into drive A, and enter A: to change the default to drive A.

2. Enter QUEMS to run the QUEMS data acquisition software. The program will begin by asking for verification of the date and time.

3. Put the data cartridge into the translator.

4. Select initialization from the main menu.

5. The initialization menu will appear, and you will be asked to verify the date and time.

6. After proper date and time verification, the data cartridge will be erased and its internal clock set. The translator will beep continuously and the light on the data cartridge will blink.

7. The data cartridge is now initialized. Remove it from the translator.

Starting Data Collection

1. Carefully slide an initialized data cartridge into the raingauge module. Verify that the leads are properly connected between the raingauge and the raingauge module.

2. Press the button on the raingauge module. The light on the data cartridge should come on.

3. Tip the raingauge bucket ten times and observe that the light blinks with each tip.

4. Carefully replace the raingauge collector.

5. Record the start time and the starting tips in the log book.

Data Recovery

The following procedure is used to recover the information stored in the data cartridge. Begin by connecting the T1000 and the translator, and applying power to both units. The T1000 will go through the boot-up process; when this has finished the C> prompt will be displayed.

1. Manually tip the raingauge bucket ten times while watching to see that the light on the data cartridge blinks at each tip.

2. Press the button on the raingauge module. The light should come on while the button is depressed.

3. Carefully remove the data cartridge from the raingauge module, being mindful not to press the module button.

4. Put the QUEMS/data disk into drive A, and enter A: to change the default to drive A.

5. Enter QUEMS to run the QUEMS data acquisition software. The program will begin by asking for verification of the date and time.

6. The main menu is displayed first. Select the download option.

7. The download screen will appear, with an empty table titled:
TEMP NO STN NO START DATE/TIME FINISH DATE/TIME MINS WARNINGS

8. At this point the program is waiting for data. Insert the data cartridge into the translator. **The data cartridge should not be put into the translator prior to this point,** since the download program recognizes the insertion of the cartridge.

9. The translator will emit a short beep, the message 'fetching data' will flash quickly at the bottom of the screen, and an entry in the table will appear showing the station number, and the start and stop times of the data. The 'mins' column represents the difference between the T1000 clock and the raingauge module clock. Large differences may be indicative of errors in setting the T1000 clock. The warnings column can have one or more of the following codes indicating specific conditions:

G A data **gap** has been detected. This occurs when the start time of this data is later than the stop time of the last data collected for the station. This condition will almost always occur, since the data cartridge will be out of the raingauge module for at least as long as is necessary to download the data and initialize the cartridge for the next period.

O **Overlapping** data has been detected. This can be due to errors in setting the clock. Usually this is not too serious.

M Indicates a low raingauge module battery.

C Indicates a low data cartridge battery.

S Clock staus bit not set. This indicates that the rainguage module was unable to access the data cartridge.

10. Inspect the download screen and verify that the information is reasonable. Enter the information in the log book.

11. Type **X** to exit the downloading procedure. Two hourly totals for the current date will be displayed. Verify that the data appear reasonable.

12. Enter a **q** to exit the validation screen.

13. You will be prompted 'Validation OK ?'. Enter **y**.

14. Station number n not validated... will appear next. Type **P** to proceed.

15. If there were entries in the warnings column, you will be asked if the data is to be edited. Enter **N** to retain the data as it is.

16. At this point the final data file will be written and the program will return to the main menu. If for some reason it appears that the data was not archived properly to disk, the download process can be repeated. However, the download program may not be able to automatically read the data from the cartridge on a second try. This arises because the cartridge has an internal flag which is set after a data download which indicates that the cartridge has already been read. This flag can be

it becomes obvious that the data will not download automatically.

Creating a New Data Diskette

Begin by applying power to the T1000. The computer will go through the boot-up process; when this has finished the C> prompt will be displayed.

1. Put the NEW_DISK 5 1/4" diskette in the external floppy drive.

2. Enter **b:** to change the default drive to b:.

3. Enter **NEW_DISK** to begin the procedure. Follow the instructions to create a blank 3 1/2" diskette. The procedure will also copy the necessary software and data files to the new data disk.

Transferring the Data to Virginia

1. Use the DOS format command to format a new 5 1/4" disk in drive b:

2. Use the DOS copy command, or the DS program (see DS.DOC on the Misc Software disk), to copy the station data files to the 5 1/4" disk. Also copy the **flags.dat, store.dat** and **sitelist.dat** data files.

3. Mail the diskette to Virginia.

Toshiba Comms Connection

Toshiba COMMS port pin #	Signal name	DIrection	DB-25 (female)
1	DCD	<-------	8
2	RD	<-------	3
3	SD	------->	2
4	DTR	------->	20
5	GND	<------->	7
6	DSR	<-------	6
7	RTS	------->	4
8	CTS	<-------	5
9	RI	<-------	22

Site Number:______
Site Name:______________________

Date	Time (1st)	Action (start, stop, dwnld)	Log. #	Data Cart. #	Valid. OK? (y/n)	Tips	Comments

Appendix II

Florida Precipitation Data

Keeping in mind the prime objective of the TRMM project, the purpose of analyzing the land-surface precipitation measurements is to obtain a measurement of rainfall (i.e., a representative areal average) that will provide a 'ground truth' for the Florida peninsula on the time and space scales of interest to the project. This, in turn, will be used in calibrating the remote sensing equipment. The critical need of all indirect estimation or measurement schemes is the acquisition of a high quality ground truth data set.

It is proposed that the ground truth data base is built upon the existing NCDC point measurements and extended to incorporate all the catchment and watershed area networks, as well as the mesonetwork of automated stations located in the vicinity of the Kennedy Space Center. It is from this multi-temporal scale data base (i.e., 1-min, 15-min, hourly and daily measurements) that a spatially smoothed time series of monthly precipitation will be obtained.

Initial analysis of the rainfall data collected over the Florida peninsula will be based on the NCDC data, namely the daily cooperative stations, hourly recording locations and the 15-min records. The reason for looking more closely at these data sets before extending the data base to encompass all the other networks, is that the NCDC data already totals hundreds of thousands of records. This in itself requires a well planned approach to handling the data. The data is also quality checked and appropriately flagged for missing or unreliable information, etc.

Statistics derived from the long term historical records are important for comparing the short term averages. Thomas (1970) suggests that a minimum record length of seven years is necessary to provide a meaningful statistic. The multi-faceted network of direct and indirect measurements may be fully operational for this period of time prior to the TRMM mission. This should then provide adequate statistics concerning the monthly areal rainfall distribution. But there are other aspects deserving consideration, namely:

a) wet and dry years and their significant effect on rainfall totals. 'Wet years sometimes doubling the amounts received during a dry year.' (Bradley, 1972)

b) determining the start and end of the rainy season. 'The season has begun as soon as early May and has been delayed as late as June.' (Bradley, 1972)

c) differentiating areas prone to thunderstorms from those areas of less frequent occurrence.

d) tropical disturbances - identify the occurrence of hurricanes and their contribution to the rainfall totals. Hurricanes and tropical storms contribute about 7% of the annual rainfall. (Brandes, 1981)

These aspects lead on to queries concerning the long term records:

1) the possibility of long term changes, and

2) cyclic changes and their return frequencies.

These considerations should be taken into account when determining the natural variability as well as producing areal precipitation amounts that will relate to the swath coverage planned for TRMM.

A brief summary of relevant climatological investigations for this region is as follows:

CROWE, M., REEK, T. and MATTINGLY, R., 1988

NCDC Automated Graphics: Each state is divided into climatological divisions of homogeneous climatological characteristics. The station data are then 'space' averaged and divisional statistics are published and archived (Fig. 1). As well as the digitized data, the National Weather Center provides a selection of maps based on the Cooperative station network. These maps for each station include monthly and seasonal rainfall departures from the 30 year norm (Fig. 2).

Graphical system compares current monthly statistics with the historical records using individual station and divisional averages for each state. The graphics provide an historical record and an areal distribution.

The historical perspective is based on a 30-year normal based on records from 1951-1980 or from 1941-1970.

Cluster analyses are also depicted in bar graph form with no area within the state representing more than 40% of the total region (Fig. 3).

Time series of monthly departures from the normal rainfall as percentages are prepared for each cluster as well as running means (Fig. 4).

This graphical presentation has only been initiated since January 1987.

SCHWARTZ, B.E. and BOSART, L.F., 1979

Diurnal variability of Florida rainfall is analyzed on a monthly basis using hourly rainfall for 68 stations over the time period 1942-1972.

Rain measurements are made to the nearest 0.25 mm and are divided into three categories: > 0.25 mm; > 2.5 mm and > 10 mm. Three month seasonal and annual analyses were also performed to give an overview of the diurnal variation.

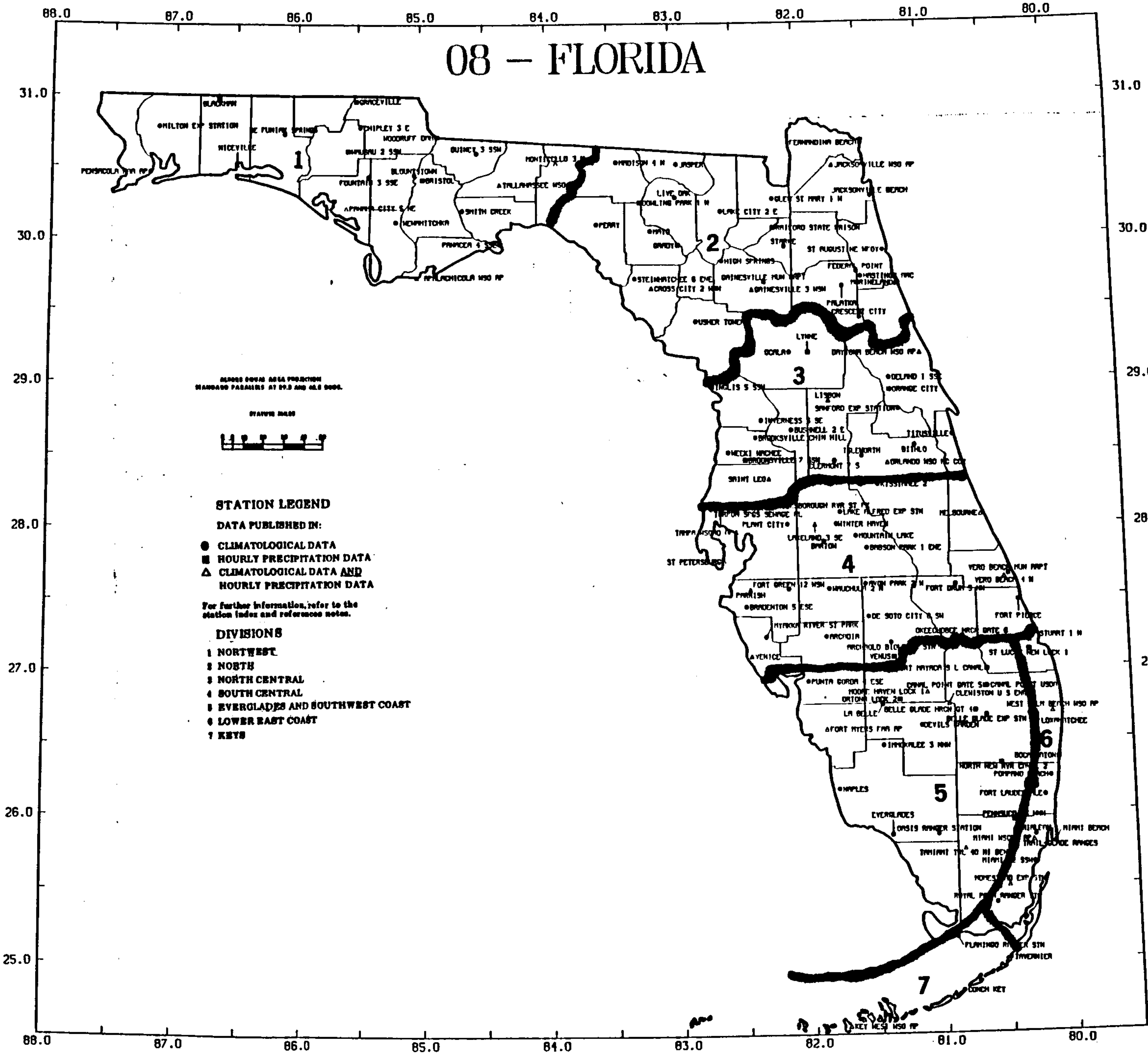

Figure 1. The State of Florida.

Figure 2.

MONTHLY PRECIPITATION DEPARTURE FROM INDIVIDUAL STATION NORMALS (1951–1980)

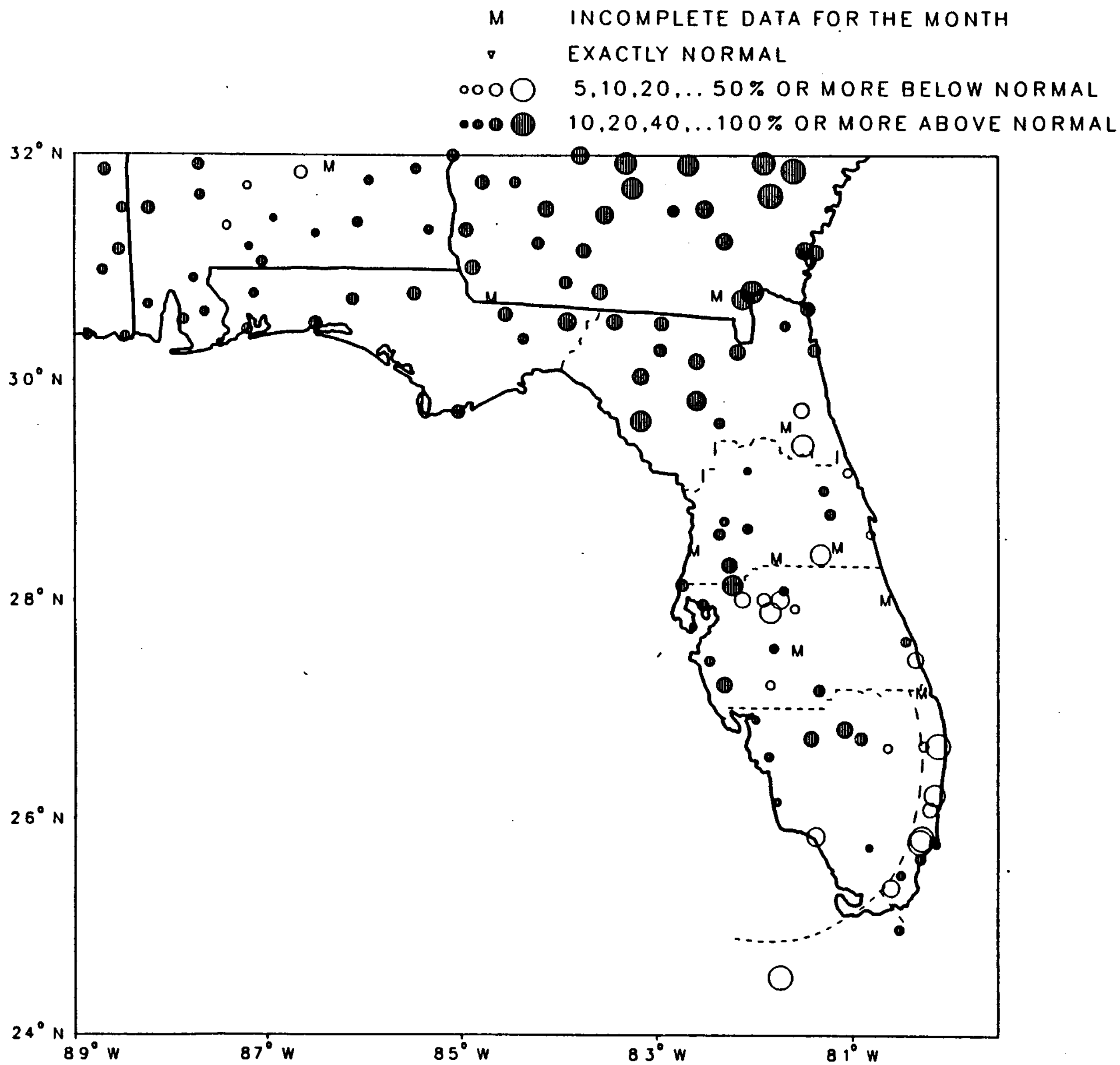

CIRCLE DIAMETER IS PROPORTIONAL TO DEPARTURE ON A CONTINUOUS SCALE

Figure 3.

MEAN MONTHLY PRECIPITATION FREQUENCY DISTRIBUTION FOR PERIOD OF RECORD 1931–1987 FOR MONTH OF JANUARY FLORIDA

CLUSTER 1 –DIVISION(S):
NORTHWEST 01
NORTH 02

CLUSTER 2 –DIVISION(S):
NORTH CENTRAL 03
SOUTH CENTRAL 04

CLUSTER 3 –DIVISION(S):
EVERGLADES AND SW COAST 05
LOWER EAST COAST 06

CLUSTER 4 –DIVISION(S):
KEYS 07

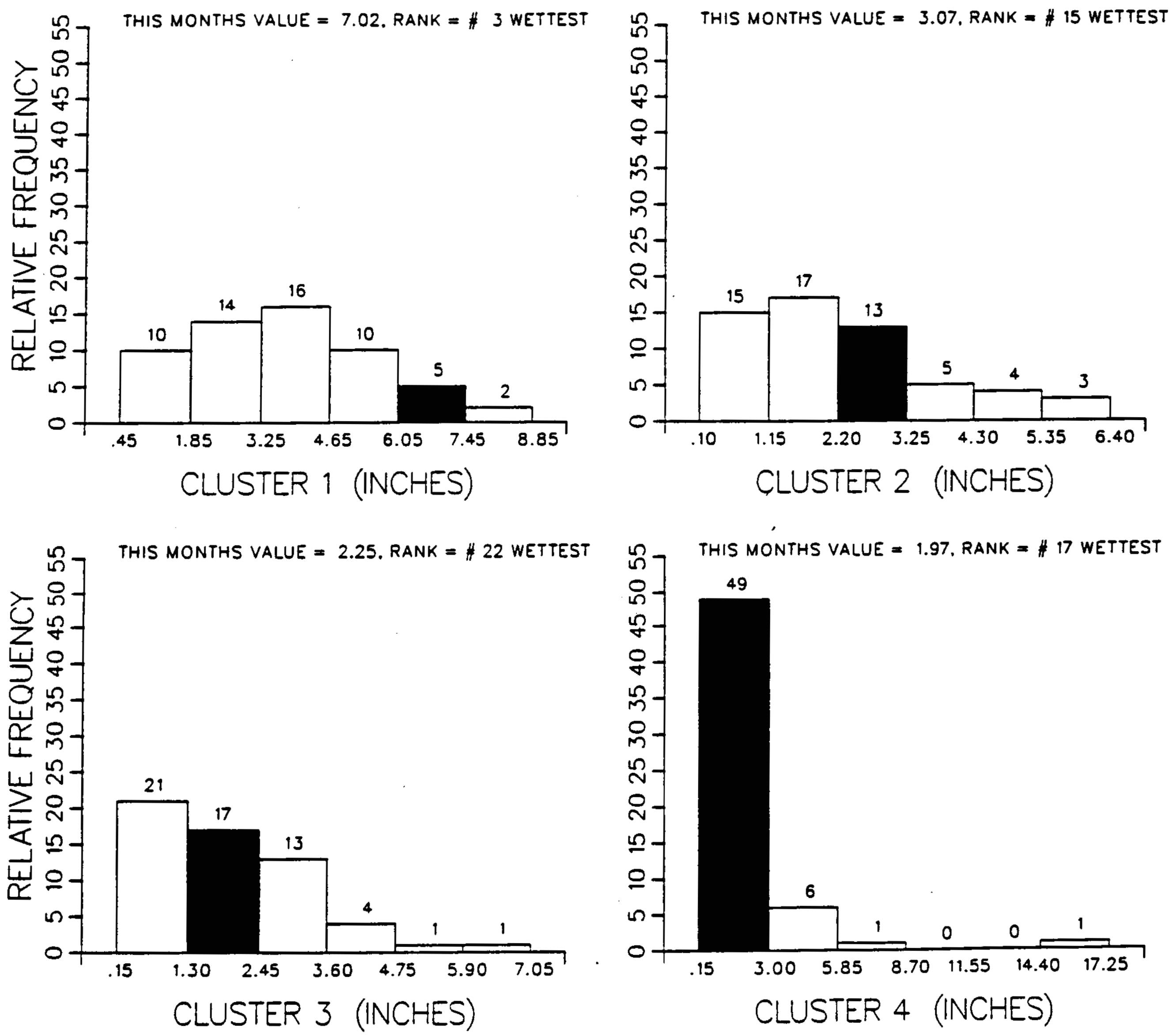

ORIGINAL PAGE IS
OF POOR QUALITY

Figure 4.
PRECIPITATION DEPARTURES FROM NORMAL (1951–1980)
FOR THE 49 MONTHS
ENDING JANUARY 1987
FLORIDA

CLUSTER 1 –DIVISION(S):
NORTHWEST 01
NORTH 02

CLUSTER 2 –DIVISION(S):
NORTH CENTRAL 03
SOUTH CENTRAL 04

CLUSTER 3 –DIVISION(S):
EVERGLADES AND SW COAST 05
LOWER EAST COAST 06

CLUSTER 4 –DIVISION(S):
KEYS 07

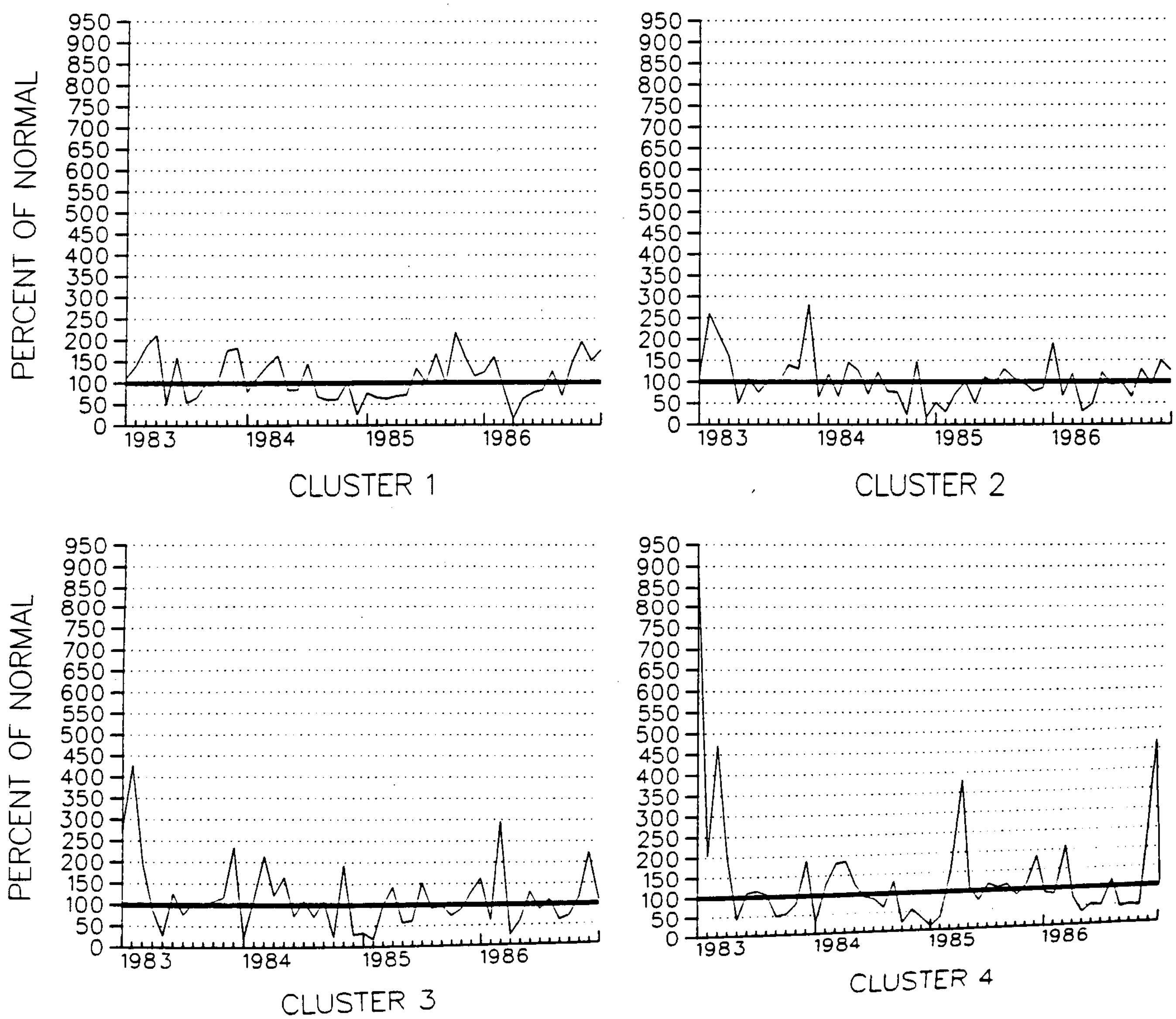

The percentage of probability of precipitation at specific stations is also presented.

Technique: harmonic analysis and normalized amplitude and phase for the diurnal and semi-diurnal cycles are prepared for each of the rain rate categories.

Presentation of data is as seasonal maps in vectorial format and depicting first harmonics (Figs. 5a and 5b).

Deficiencies of research: prevailing wind direction considered important in terms of the timing and onset of the rain over the peninsula but not considered in this study.

Reference also made to the importance of small scale variation due to topography and sea breeze circulation.

<u>WALLACE, J.M., 1975</u>

Hourly data on frequency of four rain events generated statistics on amplitude and phase of diurnal and semi-diurnal cycles at each station. This was the method employed by Schwartz and Bosart.

Amplitude and phase angle gave insight into the importance of thermodynamical processes (affecting the stability parameter) and the dynamic processes (influencing mass convergence) as factors controlling the frequency and intensity of convective activity.

Reasoning for strong diurnal rain pattern over Florida:

> timing of maximum low level convergence and maximum convective activity suggest convective precipitation controlled almost entirely by dynamical processes. The severity of convection being influenced by the thermodynamic processes.

<u>THOMAS, T.M., 1970</u>

A summary of the historical climatological records of southern Florida covering the period 1825-1968 and covering the area south of latitude 29°N. Rainfall records were obtained for 157 stations from a number of reference sources:

> Smithsonian World Weather Records, Vol. 79;
> Climatic Summary of the United States Weather Bureau Bulletin W. '1912';
> U.S. Weather Bureau Climatological data of Florida.

From the statistical analyses, single monthly time series records varying from 50 to 70 years in length display the geographical distribution of the rainfall variable (Fig. 6).

The complexity of the spatial distribution within any one month was illustrated in a series of similar figures.

Figure 5. Normalized amplitude (a) indicated by vectors and phase of the diurnal cycle in the total frequency of precipitation (December-February). (b) As a percentage of the first harmonic of the yearly cycle (after Schwartz and Bosart, 1979).

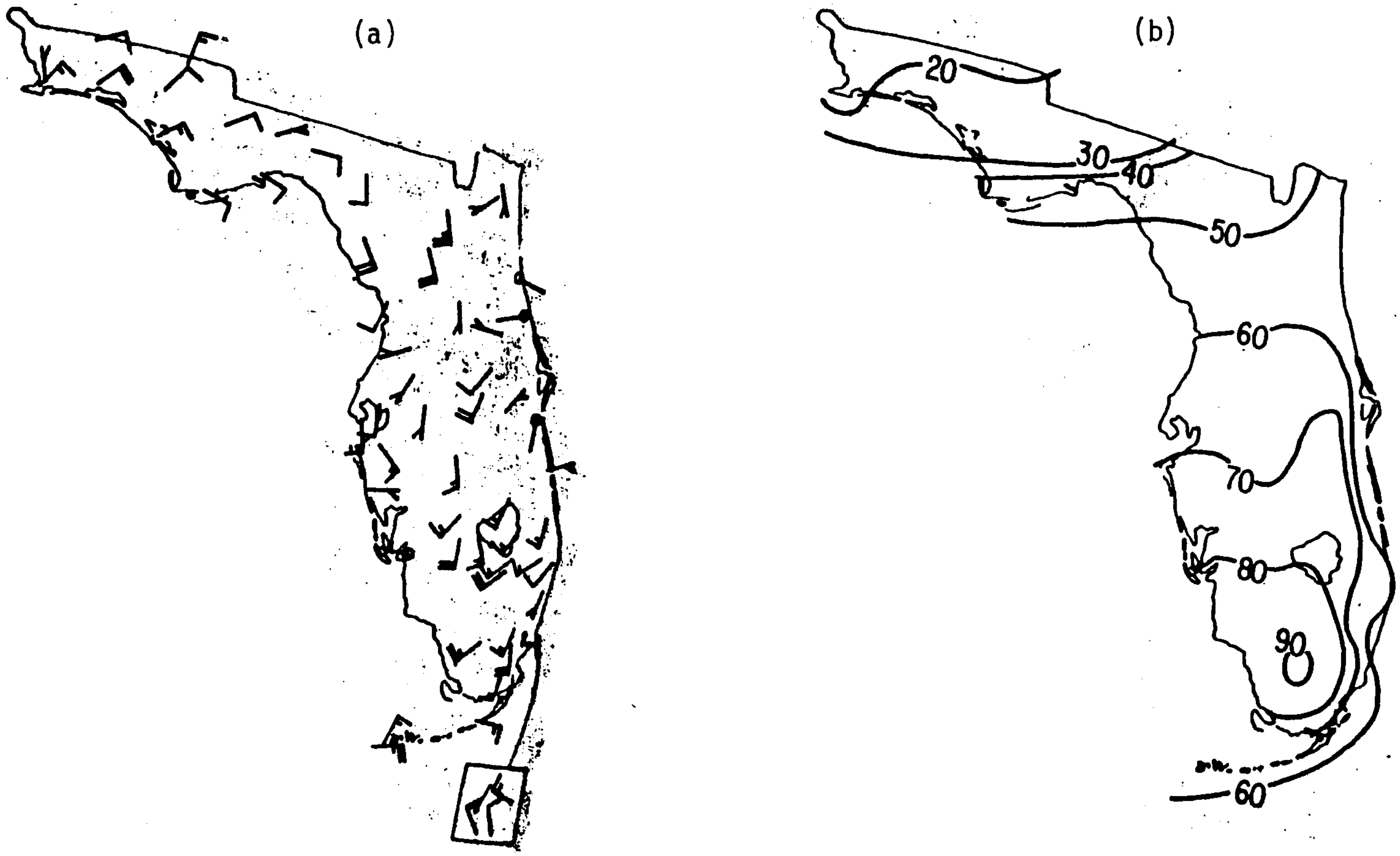

ORIGINAL PAGE IS
OF POOR QUALITY

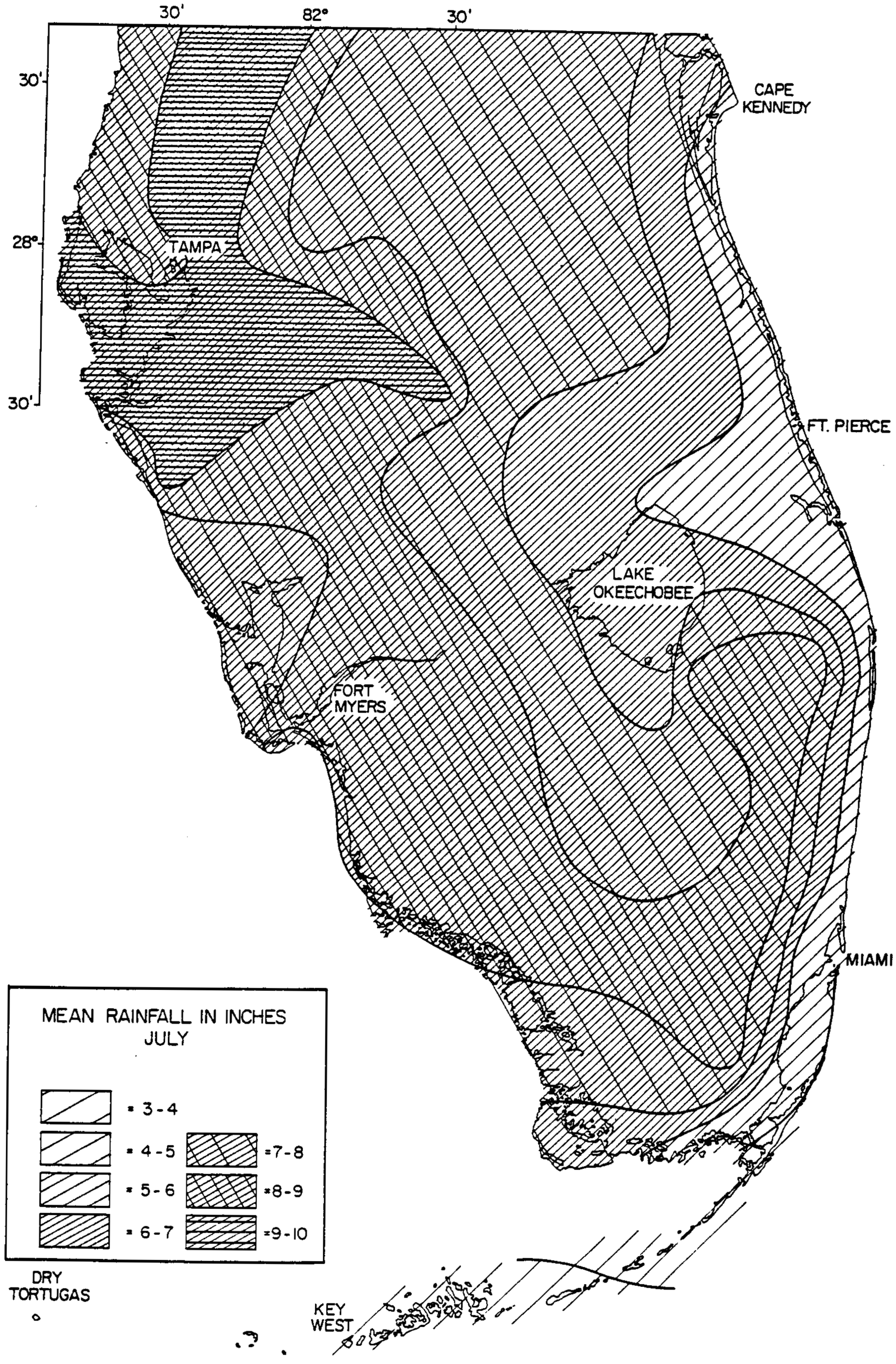

Figure 6. Average July rainfall in inches. Isohyets are drawn in 1" increments (after Thomas, 1970).

Single linear time series were calculated using data contained within areas of equal annual rainfall within 5 inch intervals (i.e., 35-40 in., 40-45 in., ...60-65 inches/year) (Fig. 7).

The rainfall distribution exhibits a bimodal characteristic of two wet periods per year. From the power spectral analysis, a return frequency of about five years was predicted along the eastern coastline and Florida Keys but it did not extend inland. Other studies suggested a 25-year return period.

General Approach

All statistics are to include totals, number of observations, means, standard deviations, variances and coefficients of variance.

It is intended that by undertaking the following analyses, one will gain an in-depth appreciation for the variability of the rainfall over the entire Florida peninsula. Most investigations todate have focussed on southern portion of the peninsula. It is hoped that by undertaking the present task in this rather laborious manner, will ultimately lead to a reduction in the error factor when determining the areal precipitation over the thirty day period as prescribed for the TRMM project.

A listing of rainfall stations for each NCDC data set is tabulated giving station ID number, name, latitude and longitude (Table 1). The first parameter is required for identifying stations on tape; the station name will aid a manual observer in perusing printouts and the lat/long are necessary for plotting the values on the state outline map. This last task will then be extended into contouring the data to create isohyetal maps. Some stations have not as yet been identified according to their station number, hence the blank spaces in the station file listing.

Those stations that have had several recording periods over the years due to slight changes in instrument location, etc., require closer inspection to verify whether data files overlap; are complimentary and so on. Certain station files may be able to be merged together giving a longer record and also reducing the bulk of the stations located in very close proximity. This latter aspect may cause problems in the plotting programs if not dealt with at this point in time.

Without giving a step-by-step account of how the rainfall data is to be processed, it is intended that a long term data base with respect to the best areal coverage, i.e., gauge density, will be determined from the daily cooperative stations. From this baseline, the summer convective rainfall period will be identified taking into account the spatial variation over the peninsula. The hourly rainfall data will then be analyzed on this basis giving hourly averages per station, areal hourly averages and percentages of the total annual rainfall. These diurnal patterns should highlight further spatial variation which can then be considered at the higher resolution of 15-min rainfall records. The focus will then move from the spatial plane to the temporal level where intense convective rain events produce the significant rainfall.

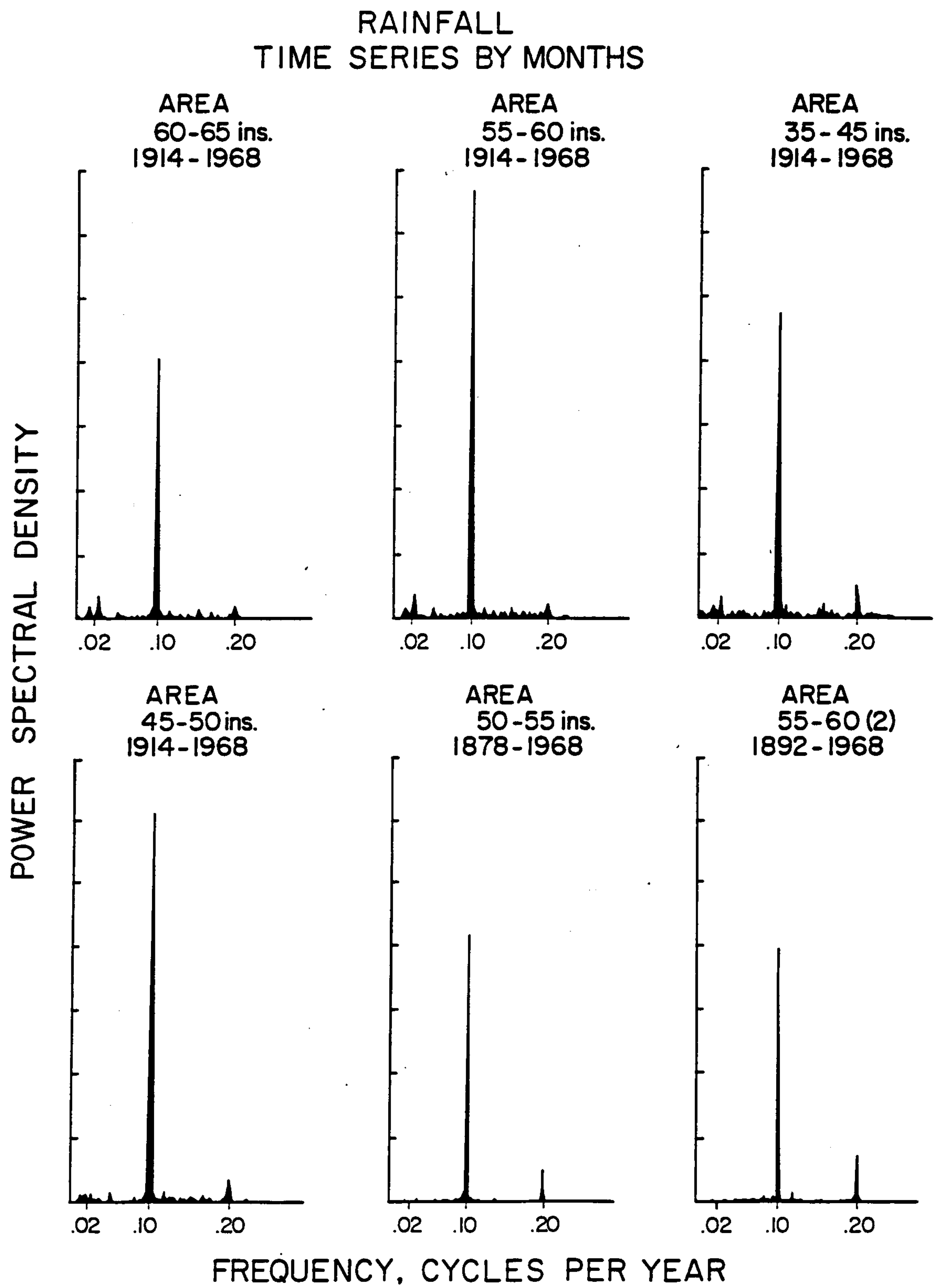

Figure 7. Return frequencies of cyclic behavior in rainfall (0.02 = 5 years; 0.1 = 1 cycle/year; 0.02 = 2 cycles/year) (after Thomas, 1970).

TABLE 1.

Listing of NCDC rainfall stations on the Florida peninsula.

DAILY COOPERATIVE STATIONS IN THE STATE OF FLORIDA

STN ID	STN NAME	LAT	LONG
080070	ALEXANDER SPRINGS	2905	8134
080228	ARCADIA	2714	8151
080236	ARCHBOLD	2711	8121
080369	AVON PARK	2736	8121
080390	BABSON PARK	2751	8131
080478	BARTOW	2754	8151
080520	BAY LAKE	2804	8230
080535	BAYPORT	2832	8239
080540	BAYPORT	XXXX	XXXX
080611	BELLE GLADE	2640	8038
080739	BIG CYPRESS	2619	8100
080758	BITHLO	2833	8107
080845	BOCA RATON	2622	8005
080887	BONITA SPRINGS	2620	8145
080940	BRADENTON	2729	8233
080945	BRADENTON	2727	8228
081046	BROOKSVILLE	2837	8222
081163	BUSHNELLS	2840	8205
081218	CAMP BLANDING	2959	8159
081271	CANAL POINT	2652	8038
081276	CANAL POINT	2652	8038
081305	FLAMINGO	2509	8056
081310	CAPTIVA	2632	8211
081432	CEDAR	2908	8302
081632	CLEARWATER	2759	8247
081635	CLEARWATER	2759	8250
081641	CLERMONT	2829	8147
081649	CLEWISTON	2645	8055
081654	CLEWISTON	2645	8055
081716	COCONUT GROVE	2539	8017
081795	CONCH KEY	2447	8053
081869	CORNWELL	2724	8110
081978	CRESCENT CITY	2925	8130
082008	CROSS CITY	2939	8310
082011	CROSS CITY	2958	8306
082114	DANIA	2604	8012
082150	DAYTONA BEACH	2913	8102
082158	DAYTONA BEACH	2911	8103
082200	DEER PARK	2806	8054
082229	DELAND	2901	8114
082288	DE SOTO	2722	8131
082298	DEVILS GARDEN	2636	8108
082418	DRY TORTUGAS	2438	8252
082827	EUSTIS	2850	8141
082834	EVA	2823	8149
082850	EVERGLADES	2551	8123
082915	FEDERAL POINT	2945	8132
082936	FELLSMERE	2746	8041
082944	FERNANDINA	3040	8127
083020	FLAMINGO	2509	8056
083137	FORT DRUM	2735	8051

ORIGINAL PAGE IS
OF POOR QUALITY

Table 1 (cont.)

DAILY COOPERATIVE STATIONS IN THE STATE OF FLORIDA

083153	FORT GREEN	2734	8208
083163	FORT LAUDERDALE	2606	8012
083168	FORT LAUDERDALE	2607	8007
083171	FORT LAUDERDALE	2606	8014
083186	FORT MYERS	2635	8152
083207	FORT PIERCE	2728	8021
083316	GAINSVILLE	2939	8121
083321	GAINSVILLE	2938	8221
083326	GAINSVILLE	2941	8216
083470	GLEN ST MARY	3016	8211
083571	SHADY OAK	2749	8113
083840	HART	2823	8111
083674	HASTING	2943	8130
083909	HIALEAH	2550	8017
083956	HIGH SPRING	2950	8236
083986	HILLSBOROUGH RIVER	2809	8214
084075	HOLOPAW	2811	8105
084091	HOMESTEAD	2530	8030
084210	IMMOKALEE	2628	8126
084242	INDIAN LAKE	2748	8121
084262	INDIANTOWN	2701	8028
084289	INVERNESS	2850	8220
084327	ISLAND GROVE	2927	8208
084332	ISLEWORTH	2829	8137
084358	JACKSONVILLE	3030	8142
084366	JACKSONVILLE	3017	8124
084393	JASPER	3031	8257
084394	JASPER	3031	8257
084518	KENDALL	2541	8017
084570	KEY WEST	2433	8145
084575	KEY WEST	2433	8148
084620	KISSIMMEE	2818	8125
084625	KISSIMMEE	2817	8125
084662	LA BELLE	2645	8126
084707	LAKE ALFRED	2806	8143
084731	LAKE CITY	3011	8236
084771	LAKE HIAWASSEE	2832	8128
084797	LAKELAND	2801	8155
084845	LAKE PLACID	2717	8123
084866	LAKE TRAFFORD	2626	8129
084980	LEESBURG	2849	8152
085035	LIGNUMVITAE	2454	8042
085076	LISBON	2852	8147
085099	LIVE OAK	3017	8258
085124	LONGBOAT	2725	8240
085183	LOXAHATCHEE	2641	8016
085275	MADISON	3032	8326
085351	MARATHON	2443	8105
085539	MAYO	3003	8310
085607	MELBOURNE	XXXX	XXXX
085612	MELBOURNE	2804	6037
085622	MELROSE	2942	8203
085643	MERRITT ISLAND	2821	8042
085653	MIAMI	2547	8011

Table 1 (cont.)

DAILY COOPERATIVE STATIONS IN THE STATE OF FLORIDA

085658	MIAMI BEACH	2547	8008
085663	MIAMI ARPT	2548	8018
085668	MIAMI WSO	2547	8011
085678	MIAMI SSW	2539	8018
085719	MILES CITY	2611	8121
085895	MOORE HAVEN	2650	8105
085973	MOUNTAIN	2756	8136
086065	MYAKKA RIVER	2714	8219
086078	NAPLES	2610	8147
086210	NEW SMYRNA	2905	8057
086251	NITTAW	2756	8100
086318	NORTH NEW RIVER	2633	8043
086323	NORTH NEW RIVER	2620	8032
086404	OASIS	2748	8112
086406	OASIS	2551	8102
086414	OCALA	2912	8205
086419	OCALA	2913	8207
086480	OKEECHOBEE	2714	8059
086485	OKEECHOBEE	2713	8048
086628	ORLANDO	2826	8120
086633	ORLANDO WP	2833	8121
086638	ORLANDO ARPT	2833	8120
086657	ORTONA	2647	8118
086753	PALATKA	2939	8139
086880	PARRISH	2734	8226
087020	PERRINE	2536	8021
087025	PERRY	3006	8336
087033	PERRINE	2536	8021
087205	PLANT CITY	2801	8208
087254	POMPANO BEACH	2614	8009

Table 1 (cont.)

DAILY COOPERATIVE STATIONS IN THE STATE OF FLORIDA

DAILY COOPERATIVE STATIONS IN THE STATE OF FLORIDA

STN ID	STN NAME	LAT	LONG
087293	PORT MAYACA	2659	8037
087395	PUNTA GORDA	2556	8203
087397	PUNTA GORDA	2655	8159
087422			
087435			
087440	RAIFORD STATE PRISON	3004	8211
087760	ROYAL PALM RANGER STN	2523	8036
087812	ST AUGUSTINE	2954	8119
087820	ST AUGUSTINE BEACH	2950	8116
087826	ST JOHN	2954	8119
087851	ST LEO	2820	8216
087859	ST LUCIE	2705	8018
087886	ST PETERSBURG	2746	8238
087977	SANFORD	2849	8115
087982	SANFORD EXPT STN	2848	8114
088021	SARASOTA	2721	8232
088024	SARASOTA	XXXX	XXXX
088094			
088165	SHADY OAK	2749	8113
088396	SOUTH MIAMI	2545	8020
088527	STARKE	2956	8206
088565	STEINHATCHEE	2943	8318
088620	STUART	2713	8015
088671	SUNNILAND	2616	8121
088775	TAMIAMI	2546	8027
088776			
088780	TAMIAMI TRAIL	2545	8050
088788	TAMPA	2758	8232
088811			
088824	TARPON SPRINGS	2809	8245
088841	TAVERNIER	2501	8031
088885			
088942	TITUSVILLE	2837	8050
088967			
089048	TURKEY HAMMOCK	2748	8111
089120	USHER TOWER	2925	8249
089176	VENICE	2706	8226
089184	VENUS	2702	8121
089214	VERO BEACH	2739	8025
089219	VERO BEACH	2738	8027
089401	WAUCHULA	2734	8149
089430	WEEKI WACHEE	2831	8235
089520			
089520	WEST PALM BEACH	2643	8003
089521			
089525	WEST PALM BEACH	2641	8006
089535			
089707	WINTER HAVEN	2801	8145

Table 1 (cont.)

HOURLY PRECIPITATION STATIONS IN THE STATE OF FLORIDA

HOURLY PRECIPITATION STATIONS IN THE STATE OF FLORIDA

STN ID	STN NAME	LAT	LONG
080369	AVON PARK	2736	8121
080374	AVON PARK	XXXX	XXXX
080616	BELLE GLADE	2642	8043
080739	BIG CYPRESS	2619	8100
080758	BITHLO	2833	8107
080845	BOCA RATON	2622	8005
080975	GRADY	2958	8254
081046	BROOKSVILLE	2837	8222
081048	BROOKSVILLE	2828	8227
081271	CANAL POINT	2652	8038
081565	BITHLO	XXXX	XXXX
081649	CLEWISTON	2645	8055
081654	CLEWISTON	2645	8055
081983	XXXXXXX	XXXX	XXXX
082008	CROSS CITY	2939	8310
082011	CROSS CITY	2958	8306
082158	DAYTONA BEACH	2911	8103
082200	DEER PARK	2806	8054
082391	DOWLING PARK	3016	8317
082659	VALPARAISO ELGIN AFB	XXXX	XXXX
082923	FELDA	2632	8126
083137	FORT DRUM	2735	8051
083186	FORT MYERS	2635	8152
083316	GAINSVILLE	2939	8121
083321	GAINSVILLE	2938	8221
083543	GRADY	2957	8257
083571	SHADY OAK	2749	8113
083909	HIALEAH	2550	8017
084075	HOLOPAW	2811	8105
084091	HOMESTEAD	2530	8030
084242	INDIAN LAKE	2748	8121
084273	INGLIS	2902	8241
084358	JACKSONVILLE	3030	8142
084371	JACKSONVILLE	XXXX	XXXX
084393	JASPER	3031	8257
084518	KENDALL	2541	8017
084570	KEY WEST	2433	8145
084575	KEY WEST	2433	8148
084620	KISSIMMEE	2818	8125
084625	KISSIMMEE	2817	8125
084636	OASIS FISHING LODGE	2748	8112
084667	LA BELLE	XXXX	XXXX
084707	LAKE ALFRED	2806	8143
084712	LAKE ALFRED	XXXX	XXXX
084731	LAKE CITY	3011	8236
084797	LAKELAND	2801	8155
084980	LEESBURG	2849	8152
085035	LIGNUMVITAE	2454	8042
085076	LISBON	2852	8147
085182	LOXAHATCHEE	2641	8016
085237	LYNNE 4 SE	2910	8152
085391	MARINELAND	2940	8113

Table 1 (cont.)

HOURLY PRECIPITATION STATIONS IN THE STATE OF FLORIDA

085607	MELBOURNE	XXXX	XXXX
085612	MELBOURNE	2804	8037
085658	MIAMI BEACH	2547	8008
085663	MIAMI ARPT	2548	8018
085668	MIAMI WSO	2547	8011
085719	MILES CITY	2611	8121
085895	MOORE HAVEN	2650	8105
086078	NAPLES	2610	8147
086318	NORTH NEW RIVER	2633	8043
086323	NORTH NEW RIVER	2620	8032
086404	OASIS	2748	8112
086419	OCALA	2913	8207
086485	OKEECHOBEE	2713	8048
086584	ORANGE CITY	2857	8118
086628	ORLANDO	2826	8120
086638	ORLANDO ARPT	2833	8120
086657	ORTONA	2647	8118
086880	PARRISH	2734	8226
087293	PORT MAYACA	2659	8037
087440	RAIFORD STATE PRISON	3004	8211
087820	ST AUGUSTINE	2951	8116
087851	ST LEO	2820	8215
087859	ST LUCIE	2705	8018
087886	ST PETERSBURG	2747	8238
088165	SHADY OAKS	2749	8113
088671	SUNNILAND	2616	8121
088775	TAMIAMI CANAL	2546	8027
088780	TAMIAMI TRAIL	2546	8050
088788	TAMPA	2758	8232
089010	TRAIL GLADE RANGES	2546	8028
089048	TURKEY HAMMOCK- OASIS	2748	8111
089176	VENICE	2706	8227
089184	VENUS	2702	8121
089214	VERO BEACH	2739	8025
089219	VERO BEACH	2738	8027
089520	WEST PALM BEACH	2643	8003
089525	WEST PALM BEACH	2641	8006

Table 1 (cont.)

15 -MIN PRECIPITATION DATA FOR THE STATE OF FLORIDA

15 -MIN PRECIPITATION DATA FOR THE STATE OF FLORIDA

STN ID	STN NAME	LAT	LONG
080845	BOCA RATON	2622	8005
081048	BROOKSVILLE	2837	8222
081654	CLEWISTON	2645	8055
082008	CROSS CITY	2939	8310
082391	DOWLING PARK	3016	8317
083186	FORT MYERS	2635	8152
083321	GAINSVILLE	2938	8221
083543	GRADY	2957	8257
084091	HOMESTEAD	2530	8030
084273	INGLIS	8250	2905
084797	LAKELAND	2801	8155
085076	LISBON	2852	8147
085391	MARINELAND	2940	8113
085612	MELBOURNE	2804	8037
085584	ORANGE CITY	2856	8118
086880	PARRISH	2734	8226
086988	PENNSUCO	2556	8027
087440	RAIFORD	3004	8211
087851	ST LEO	2820	8216
087886	ST PETERSBURG	2746	8238
088780	TAMIAMI TRAIL	2545	8050
089010	TRAIL GLADE RANGES	2546	8028
089176	VENICE	2706	8226
089184	VENUS	2704	8111
089219	VERO BEACH	2738	8027

The sensitivity of the density of the various networks has yet to be determined for the Florida area. Ultimately, with the use of a decorrelation approach in conjunction with precipitation records from key sites, it should be feasible to deploy less dense but adequate networks throughout the tropical rain belt. The procedure involving the use of an optimal estimator of areal precipitation (based on the work of Schaake, 1978), should be tested in the Florida region. It is proposed that the decorrelation expression be developed from the historical precipitation records. This estimator of rainfall at non-instrumented locations is based on an optimal weighting factor and is dependent on the coefficient of variation of point precipitation. measurements. In the Florida situation, because of the flat terrain, the decorrelation expression will be largely a function of distance.

<u>Other Aspects to be Considered</u>:

* Categorize rain days according to upper air soundings.

* Investigate the heat budget approach for estimating precipitation.

* Assess the effects of urbanization on the rainfall pattern over the years of growth and development.

* Assess impact of climatological disturbances.

* Investigate the already existing satellite relay and processing system - a data collection system (DCS) based in Miami, using LANDSAT satellite as a data relay platform in processing rainfall and water level information obtained from gauging stations in the water conservation areas, Everglades National Park and Big Cypress Swamp.

References

Bradley, J.T., 1972: The climate of Florida, in Climates of the States, Vol. 1: Eastern States, NOAA, U.S. Dept. of Commerce, 45-70.

Brandes, D., 1981: The significance of tropical cyclone rainfall in the water supply of southern Florida. PhD dissertation, University of Florida, Dept. of Geography, Gainesville, FL, 151 pp.

Crowe, M., T. Reek and R. Mattingly, 1988: Operational automated graphics at the National Climatic Data Center, Bull. Amer. Meteor. Soc., 69, 28-38.

Schaake, J.C., Jr., 1978: Accuracy of point and mean areal precipitation estimations from point precipitation data. NOAA Tech. Memo. NWS-HYDRO, 98 pp.

Schwartz, B.E. and L.F. Bosart, 1979: The diurnal variability of Florida rainfall. Mon. Wea. Rev., 107, 1535-1545.

Thomas, T.M., 1970: A detailed analysis of climatological and hydrological records of south Florida with reference to man's influence upon ecosystem evolution. Rosentiel School of Marine and Atmospheric Science, Tech. Rept. 70-2, 89 pp.

Wallace, J.M., 1975: Diurnal variations in precipitation and thunderstorm frequency over the conterminous United States. Mon. Wea. Rev., 103, 406-419.